

ISSN 2521-6368

Volume 4
Number 2
2020

Journal of Baku Engineering University

P H Y S I C S

Journal is published twice a year
Number - 1. June, Number - 2. December

An International Journal

<http://journal.beu.edu.az>

Founder

Havar Mammadov

Editor-in-chief

Niftali Qocayev

Co-Editor

Razim Bayramov

Editorial advisory board

Azer Ahmedov (Baku State University, Azerbaijan)
Cahangir Huseynov (Azerbaijan, Azerbaijan Pedagogical University)
Eldar Qocayev (Azerbaijan, Technical University)
Eldar Masimov (Azerbaijan, Baku State University)
Enver Nakhmedov (Baku Engineering University)
Eyyub Guliyev (Azerbaijan, National Academy of Sciences)
Farhad Rustamov (Azerbaijan, Institute of Physical Problems)

Gulnara Akhverdiyeva (Azerbaijan, Institute of Physical Problems)
Izzet Efendiyeva (Azerbaijan, Baku State University)
Larisa Ismayilova (Azerbaijan, Institute of Physical Problems)
Kerim Allakhverdiyev (Azerbaijan, National Aviation Academy Of Azerbaijan)
Namiq Ahmedov (Azerbaijan, Institute of Physical Problems)
Sajida Abdulvahabova (Azerbaijan, Baku State University)

International Advisory board

Ahmed Abdinov (Azerbaijan, Baku State University)
Anar Rustamov (Germany, Hote Frankfurt University)
Ali Javan (USA, Massachusetts Institute of Technology)
Adil R. Abduragimov (USA, University of California, Los Angeles)
Amrulla Mamedov (Turkey, Bilkent Universit)
Faig Mikailzade (Turkey, Gebze Technical University, Kocaeli)
Gulshen Agayeva (Azerbaijan, Institute of Physical Problems)
Irada Aliyeva (Azerbaijan, Baku State University)
Garib Murshudov (York Akademy, UK, London)
Hamed Sari-Sarrat (USA, Texas Technik University)
Eden Mamut (Romania, Black Sea Universitetes Network Center)
Elsen Veli Veliyev (Turkey, Kocaeli University)
Edil Eyvazov (Azerbaijan, Azerbaijan Pedagogical University)
Kamran T. Mahmudov (University of Lisbon, Portugal)
Kev Salihov (Tataristan, Kazan University)
Khalil Kälantär (Displays and Optical Technologies, Japan, Tokio)
Konstantin Voldemarovich Shaitan (Russia, Moskow State University)
M.Iqbal Choudhary (University of Karachi, Pakistan)
Natiq M. Atakishiyev (Universidad National Autonoma de Mexico)
Nizami Gasanliy (Middle East Technical University, Turkey)
Okta Gassumov (Azerbaijan National Academy of Sceince, Baku)

Oguz Gulseren (Bilkent University, Turkey)
Olgun Guven (Turkey, Hacettepe University)
Rasim Mamedov (Azerbaijan, Baku State University)
Rauf Jafarov (Azerbaijan, Institute of Physical Problems)
Sebahattin Tuzemen (Turkey, Ataturk University)
Sevim Akyuz (Turkey, Istanbul University)
S.V. Chernyshenko (Germany, Koblenz University)
Suleyman I. Allakhverdiev (Russian, Akademy Science, Moscow)
Svetlana Demuhamedova (Azerbaijan, Institute of Physical Problems)
Takhtasib Aliyev (METU, Ankara, Turkey)
Taleh Yusifov (University of California, USA, Los Angeles)
Tariel Ismayilov (Azerbaijan, Baku State University)
Tarlan Efendiye (Belarus, National Academy of Science)
Toshi Nagata (Japan, National Institute for Natural Science)
V. Thavasi (Singapore, National University of Singapore)
Vanin A.F. (Russia, National Academy of Science)
Vagif Nasirov (Azerbaijan, Azerbaijan Pedagogical University)
Vladimir Pashenko (Russia, Moskow State University)
Veli Gusseynov (National Academy of Science, Baku, Azerbaijan)
Vladimir Gorbarchuk (Poland, Lyubel Polytechnic University)
Yusuf Sahin (Turkey, Ataturk University)

Executive Editors

Shafag Alizade

Assistant Editors

Ulker Agayeva

Lala Hajiyeva

Design

Ilham Aliyev

Contact address

Journal of Baku Engineering University
AZ0102, Khirdalan city, Hasan Aliyev str. 120, Absheron, Baku, Azerbaijan
Tel: 00 994 12 - 349 99 95 Fax: 00 994 12 349-99-90/91

e-mail: jr-physics@beu.edu.az

web: <http://journal.beu.edu.az>

facebook: [Journal Of Baku Engineering University](#)

Copyright © Baku Engineering University

ISSN 2521-6368



**Journal of
Baku Engineering
University**

PHYSICS

Baku - AZERBAIJAN

Journal of Baku Engineering University

PHYSICS

2020. Volume 4, Number 2

CONTENTS

КОМПЛЕКСНАЯ ДИЭЛЕКТРИЧЕСКАЯ ПРОНИЦАЕМОСТЬ И ОПТИЧЕСКИЕ ФУНКЦИИ БИОКОМПОЗИТОВ ПЭНД+хоб.%РЧ

B.B. Салимова _____ 53

THE DECAY OF Polarized CHARGINO (NEUTRALINO) INTO HIGGS BOSONs

Abdullayev S. K., Omarova E. Sh. _____ 61

SPATIAL AND ELECTRONIC STRUCTURES OF HYLAMBATIN (8-12) PENTAPEPTIDE

G.A. Agaeva, G.R.Safarli, N.M.Godjaev _____ 76

ELECTRONIC SPECTRUM OF α -In₂Se₃ COMPOUND AND NATURE OF THE CHEMICAL BONDS

E.M. Qocayev, Z.A. Cahangirli, A.F.Garibli, S.A. Nabiyeva _____ 82

ВЛИЯНИЕ НЕОРГАНИЧЕСКИХ СОЛЕЙ НА ФАЗОВУЮ ДИАГРАММУ И РАЗДЕЛИТЕЛЬНУЮ СПОСОБНОСТЬ ВОДНОЙ ДВУХФАЗНОЙ СИСТЕМЫ ПЭГ-НАТРИЕВАЯ СОЛЬ ЛИМОННОЙ КИСЛОТЫ-ВОДА

Ә.А Масимов, Г.М Шахбазова _____ 86

THE INFLUENCE OF ETHYLENE GLYCOL AND GLYCERIN TO THE FORMATION OF AQUEOUS BIPHASIC SYSTEM POLYETHYLENE GLICOL-SODIUM CITRATE-WATER

Shahbazova Gunel Mugaddas _____ 92

CONDUCTIVE EXTENDED STATES IN Bi₂Tes<In,Cu>.

Gojayev E.M., Gahramanov A.SH., Gahramanov S.SH., Gulmammadov K.J., Mamedova S.I. _____ 97

INFLUENCE OF THE SEASHELL ON THE MECHANICAL AND ELECTRICAL STRENGTH OF HIGH PRESSURE POLYETHYLENE

E.M. Gojayev, Sh.A.Zeynalov, K.J.Gulmammadov, R.S. Ragimov, N.F. Memmedzade _____ 102

PACS. 78.20Ci; 78.30.Jw; 81.05.Lg; 82.35.Pq; 82.35.Lr.

IOT:530.1:51

КОМПЛЕКСНАЯ ДИЭЛЕКТРИЧЕСКАЯ ПРОНИЦАЕМОСТЬ И ОПТИЧЕСКИЕ ФУНКЦИИ БИОКОМПОЗИТОВ ПЭНД+хоб.%РЧ

В.В. САЛИМОВА

Сумгайитский государственный университет, г. Сумгайит

vefa_24@mail.ru

РЕЗЮМЕ

В предъявленной работе изложены результаты исследования частотной зависимости реальной и мнимой частей диэлектрической проницаемости полиэтилена низкого давления, модифицированного рыбьей чешуей. С помощью экспериментальных значений комплексной диэлектрической проницаемости, были определены оптические функции – реальные и мнимые части коэффициента преломления, оптической электропроводности, коэффициента отражения, коэффициента поглощения и потери энергии биокомпозитов ПЭНД+хоб.%РЧ.

Ключевые слова: биокомпозиты ПЭНД+хоб.%РЧ, оптические функции, комплексная диэлектрическая проницаемость, реальные и мнимые части коэффициента преломления, оптическая электропроводность.

ASPE+xhəcm%BP VİOKOMPOZİTLƏRİNİN KOMPLEKS DIELEKTRİK
KEÇİRİCİLİYI VƏ OPTİK FUNKSIYALARI

XÜLASƏ

Təqdim olunan işdə balıq pulcuqlarının modifikasiya olunmuş aşağı sıxlıqlı polietilenin dielektrik keçiriciliyinin həqiqi və xəyalı hissələrinin tezlikdən asılılıqlarının tədqiqi nəticələri təqdim edilmişdir. Kompleks dielektrik keçiriciliyinin eksperimental nəticələrindən istifadə edərək, ASPE + xəcm % BP biokompozitlərinin optik funksiyaları – sinmanın həqiqi və xəyalı əmsali, optik elektrik keçiriciliyi, əksetmə və udma əmsali, enerji itkisi müəyyən edilmişdir.

Açar sözlər: ASPE + xəcm% BP, optik funksiyalar, kompleks dielektrik keçiriciliyi, sinma əmsalının həqiqi və xəyalı hissələri, optik elektrik keçiriciliyi.

COMPLEX DIELECTRIC PERMITTIVITY AND OPTICAL FUNCTIONS
OF BIOCOMPOSITES LDPE+xvol%FS.

ABSTRACT

The presented work presents the results of studying the frequency dependence of the real and imaginary parts of the dielectric constant of high-pressure polyethylene modified with fish scales. Using the experimental values of the complex dielectric constant, the optical functions were determined - the real and imaginary parts of the refractive index, optical conductivity, reflection coefficient, absorption coefficient and energy loss of the biocomposites LDPE + xvol % FS.

Keywords: biocomposite LDPE+xvol % FS, optical functions, complex dielectric constant, real and imaginary parts of the refractive index, optical conductivity.

ВВЕДЕНИЕ

Одним из перспективных направлений металловедения является создание новых композиционных полимерных материалов. Такие материалы могут найти применение в качестве изоляции ёмкостных наполнителей энергии, работающих на импульсном напряжении. В зависимости от назначения и области применения высоковольтных импульсных устройств длительность фронта импульсов напряжения может изменяться

от нескольких десятков мс до нс. Поэтому композиционные материалы для емкостных накопителей энергии должны обладать стабильными электрофизическими характеристиками в широком диапазоне частот внешнего электрического поля. Введение наполнителя биологического происхождения существенно модифицирует структуру и свойства композиционных материалов за счет межфазных взаимодействий и образования граничного нанослоя вблизи частиц наполнителя. Это определяет особенности временного распределения локального поля, в отдельных областях полимерной системы и частотной дисперсии эффективной комплексной диэлектрической проницаемости композиционных материалов.

В этой связи при разработке композиционных материалов необходимо иметь информацию о спектре комплексной диэлектрической проницаемости самой полимерной матрицы частиц наполнителя биологического происхождения.

В свете вышеизложенного целью данной работы явилось исследование частотной зависимости комплексной диэлектрической проницаемости биокомпозитов ПЭНД+хоб.%РЧ.

МЕТОДИКА ЭКСПЕРИМЕНТА

При измерении диэлектрических параметров в качестве контакта использовалась серебряная паста. Исследование частотной зависимости диэлектрической проницаемости и угла диэлектрических потерь проводилось с использованием цифрового прибора для измерения импеданса Е7-20, как описано в [1]. Напряжение, приложенное к образцу, составляло 1 В. Погрешности измерения диэлектрической проницаемости и диэлектрических потерь составляли 3 и 5% соответственно. При исследовании температурной зависимости данная частота была принята равной 1 кГц.

ЭКСПЕРИМЕНТАЛЬНЫЕ РЕЗУЛЬТАТЫ И ОБСУЖДЕНИЕ

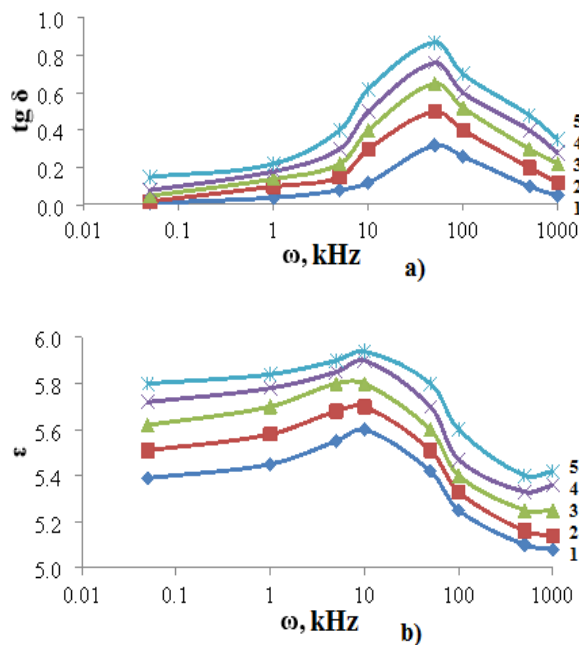


Рис.1. Частотные зависимости тангенса угла диэлектрических потерь (а) и диэлектрической проницаемости (б) биокомпозитов ПЭНД+х об%РЧ, где 1-х=3; 2-х=5; 3-х=7; 4-х=10; 5-х=15.

Результаты исследования частотной зависимости диэлектрической проницаемости и диэлектрической потери полиэтилена низкого давления, модифицированного рыбьей чешуей приведены на рис.1а, б.

На рис.1а приводятся результаты исследования частотной зависимости диэлектрической потери биокомпозитов ПЭНД+хоб%РЧ. Диэлектрическая потеря указанных биокомпозитов сначала с увеличением частоты резко увеличивается, при частоте 50 кГц достигает своего максимального значения и уменьшается. Размытый частотный спектр диэлектрической потери свидетельствует о наличии составляющих, обуславливающих различный вклад дипольно-ориентационной поляризации в общую дисперсию комплексной диэлектрической проницаемости [2-5].

Как видно, (рис. 1б) с увеличением частоты от 0.01 кГц до 1000 кГц диэлектрическая проницаемость сначала увеличивается, достигая своего максимального значения при частоте 10 Гц, а затем уменьшается. Увеличение диэлектрической проницаемости наблюдается и с увеличением объемного содержания бионаполнителя в составе полиэтилена низкого давления. Характерно для всех исследованных композитов при низких частотах происходит относительное слабое увеличение диэлектрической проницаемости, а при высоких частотах наблюдается сильное уменьшение диэлектрической проницаемости. С увеличением содержания бионаполнителя в составе композита при низких частотах происходит относительно слабое увеличение диэлектрической проницаемости.

Различный их вклад в общую дисперсию комплексной диэлектрической проницаемости обусловлен тем, что исследуемый полимер содержит полярные радикалы, а также полярные группы молекул пластификаторов. Кроме того, введение модификаторов приводит к уменьшению вязкости полимера вследствие снижения энергии межмолекулярного взаимодействия и изменению времени релаксации процессов дипольно-ориентационной поляризации полярных групп и радикалов. Полученные результаты показывают, что изменение концентрации наполнителя из рыбьей чешуи приводит к смещению частоты, релаксации всех составляющих спектра в область более низких частот, увеличению глубины или полной ширины дисперсии комплексной диэлектрической проницаемости в примерном соответствии с концентрацией наполнителя и изменению вклада отдельных составляющих спектра в дисперсию комплексной диэлектрической проницаемости.

Известно, что мерой диэлектрических потерь может служить тангенс угла δ , дополняющий угол φ до 90^0

$$\operatorname{tg} \delta = \frac{I_{\text{ак}}}{I_{\text{peak}}} = \frac{\varepsilon_i}{\varepsilon_r}$$

$I_{\text{ак}}$ и I_{peak} – активная и реактивная части силы тока.

Известно также, что обобщенная диэлектрическая проницаемость определяется формулой

$$\varepsilon^* = 1 + \frac{4\pi Ne^2}{m} \left(\frac{\omega_0^2 - \omega^2}{(\omega_0^2 - \omega^2)^2 + f^2\omega^2} - \frac{if\omega}{(\omega_0^2 - \omega^2)^2 + f^2\omega^2} \right) = \varepsilon_r - i\varepsilon_i$$

Действительная ε_r и мнимая ε_i части комплексной диэлектрической проницаемости при этом равны

$$\varepsilon_r = 1 + \frac{4\pi Ne^2(\omega_0^2 - \omega^2)^2}{m[(\omega_0^2 - \omega^2)^2 + f^2\omega^2]}$$

$$\varepsilon_i = \frac{4\pi Ne^2}{m} \frac{f\omega}{(\omega_0^2 - \omega^2)^2 + f^2\omega^2}.$$

Главный показатель преломления (вещественная часть показателя преломления) определялся по формуле

$$n = \sqrt{\frac{1}{2} \left(\varepsilon_r + \sqrt{\varepsilon_r^2 + \varepsilon_i^2} \right)}$$

Результаты расчета приведены на рис. 2. Как следует из рис.2 реальная часть коэффициента преломления при низких значениях частоты (0÷1 кГц) практически не изменяется, а в частотном диапазоне от 1 до 50 кГц наблюдается сильный рост n . С дальнейшим ростом частоты коэффициент преломления своего максимального значения достигает в частотном диапазоне 50÷100 кГц. Характер изменения коэффициентов преломления частотной зависимости исследованных биокомпозитов не отличается. С увеличением объемного содержания бионаполнителя происходит увеличение реальной части коэффициента преломления.

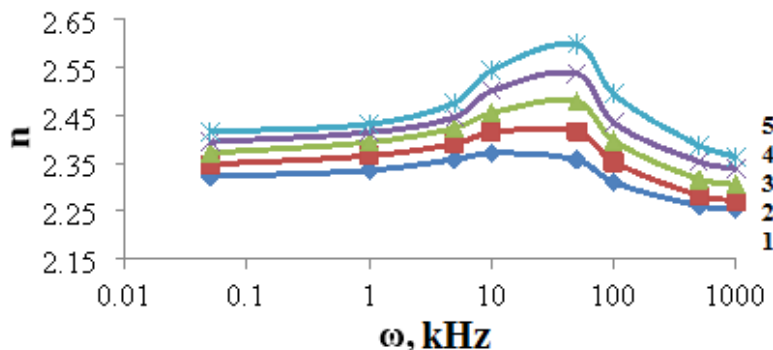


Рис.2. Частотная зависимость реальной части коэффициента преломления биокомпозитов ПЭНД+ хоб%РЧ, где 1-х=3; 2-х=5; 3-х=7; 4-х=10; 5-х=15.

Мнимая часть диэлектрической проницаемости определяется по формуле

$$k = \sqrt{\frac{1}{2} \left(-\varepsilon_r + \sqrt{\varepsilon_r^2 + \varepsilon_i^2} \right)}$$

Как следует из рис.3 частотная зависимость мнимой части коэффициента преломления имеет аналогичный характер, т. е. при низких значениях частоты наблюдается слабый рост, а в средней части коэффициент отражения достигает своего максимального значения и уменьшается.

Коэффициент отражения определяется формулой

$$R = \frac{(n - 1)^2 - k^2}{(n + 1)^2 + k^2}$$

Результаты расчета коэффициента отражения приведены на рис.4. Как следует из рис.4 в $R(\omega)$ зависимости увеличение коэффициента отражения происходит относительно сильнее. С увеличением объемного содержания рыбьей чешуи в составе полиэтилена происходит смещение максимумов в сторону высоких энергий.

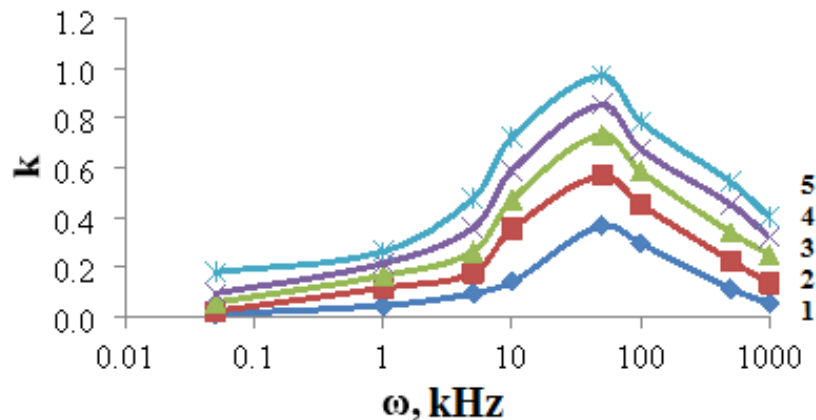


Рис.3. Частотная зависимость мнимой части коэффициента преломления биокомпозитов ПЭНД+ х об%РЧ, где 1- $x=3$; 2- $x=5$; 3- $x=7$; 4- $x=10$; 5- $x=15$.

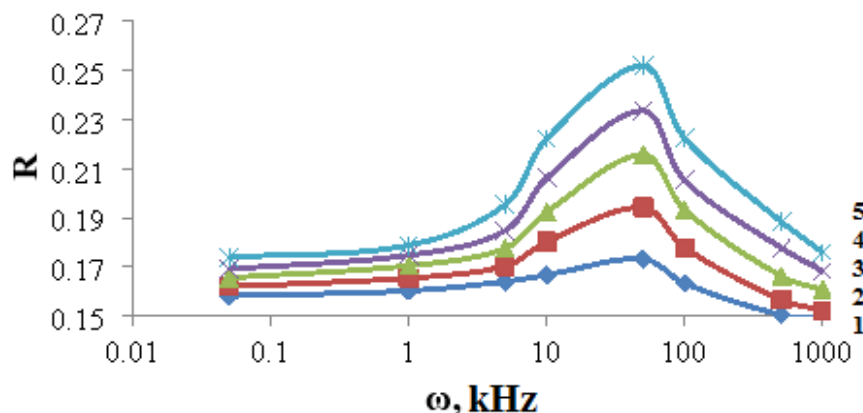


Рис.4. Частотная зависимость коэффициента отражения биокомпозитов ПЭНД+ х об%РЧ, где 1- $x=3$; 2- $x=5$; 3- $x=7$; 4- $x=10$; 5- $x=15$.

Характеристическая функция потерь энергии электронов определяется таким образом:

$$-I_m\left(\frac{1}{\varepsilon}\right) = \frac{\varepsilon_i}{\varepsilon_i^2 + \varepsilon_r^2}$$

Спектральная зависимость мнимой части обратной величины комплексной диэлектрической проницаемости представлена на рис.5. Как видно на $-I_m\left(\frac{1}{\varepsilon}\right)$ зависимостях наблюдается один максимум. Обнаружено, что при малых содержаниях бионаполнителя увеличение обратной величины комплексной диэлектрической проницаемости относительно сильная.

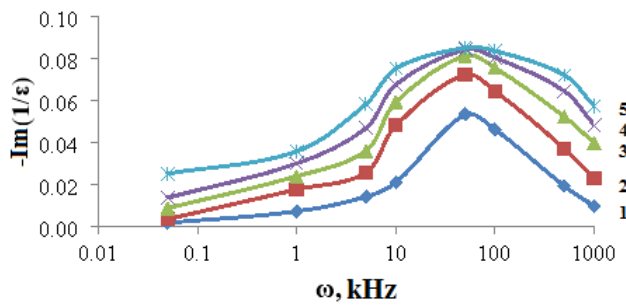


Рис.5. Частотная зависимость потерь энергии биокомпозитов ПЭНД+ хоб%РЧ, где 1- $x=3$; 2- $x=5$; 3- $x=7$; 4- $x=10$; 5- $x=15$.

Реальная и мнимая части оптической электропроводности определяется с помощью следующих формул:

$$\sigma_r = \frac{\omega \epsilon_i}{4\pi}, \sigma_i = \frac{\omega \epsilon_r}{4\pi}$$

Результаты расчета реальной и мнимой частей оптической электропроводности биокомпозитов приведены на рис.6. Как следует из рис.6 при низких частотах (0÷10 кГц) σ_r для всех исследованных биокомпозитов характерно не изменяется. Однако с увеличением частоты от 10 до 1000 кГц резко увеличивается. Мнимая часть оптической электропроводности также при низких частотах остается постоянной, а при высоких значениях частоты резко уменьшается. Интересно отметить, что мнимая часть оптической электропроводности биокомпозитов независимо от содержания бионаполнителя оказывается одинаковой.

Коэффициент поглощения определяется выражением

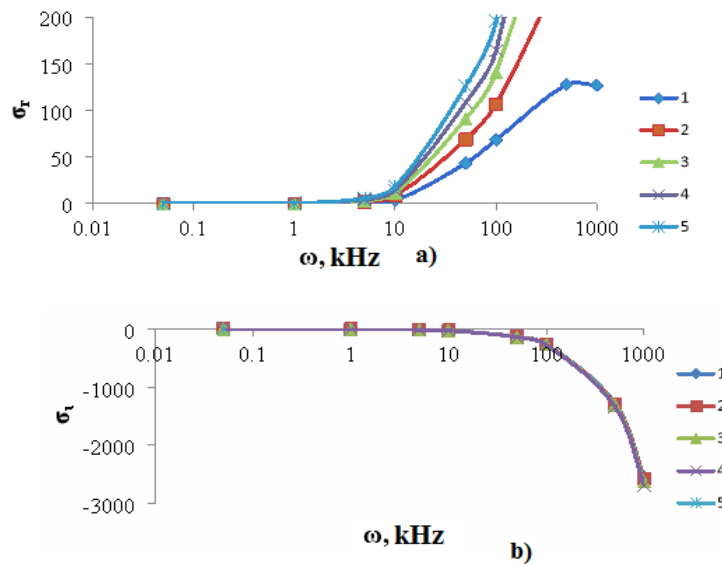


Рис.6. Частотная зависимость реальной (а) и мнимой частей (б) оптической электропроводности биокомпозитов ПЭНД+ хоб%РЧ, где 1- $x=3$; 2- $x=5$; 3- $x=7$; 4- $x=10$; 5- $x=15$.

$$\alpha(\omega) = \frac{4\pi}{\lambda} k(\omega) = \frac{2}{c} \omega k ,$$

c – скорость света в вакууме.

Как следует из рис.7 коэффициент оптического поглощения биокомпозитов при низких частотах практически не изменяется, а начиная с частоты 100 кГц увеличивается. С увеличением объемного содержания бионаполнителя в составе ПЭВД наблюдается более сильное увеличение коэффициента поглощения. Это, по-видимому, связано с тем, что с увеличением содержания наполнителя в составе происходит увеличение оптической плотности исследованных биокомпозитов [6, 7, 8].

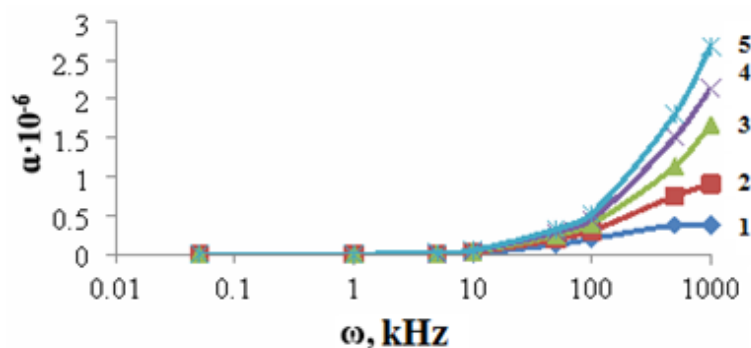


Рис.7. Частотная зависимость коэффициента поглощения биокомпозитов ПЭНД+ хоб%РЧ, где 1- $x=1$; 2- $x=2$; 3- $x=3$; 4- $x=4$; 5- $x=5$.

ЗАКЛЮЧЕНИЕ

Показано, что на основе полимера низкого давления возможно создание композиционных материалов с высоким энергосодержанием. Для получения стабильных электрофизических характеристик необходимо оптимизировать состав композиционного материала, тип и объем наполнителя. Метод диэлектрической спектроскопии в частотном ходе дает полную информацию не только о поведении комплексной диэлектрической проницаемости, но и о структуре композиционного материала, что незаменимо при целенаправленном регулировании состава компонентов и свойства композиционных диэлектриков с наполнителями биологического происхождения.

ЛИТЕРАТУРА

1. E.M.Gojayev, Sh.V.Aliyeva, X.S.Khalilova, G.S.Jafarova and S.H.Jabarov. The dielectric properties and electrical conductivity of LDPE modified by fillers of biological origin. International Journal of Modern Physics B, Vol. 33, №26, 2019, 1950309 (10 pages).
2. О.С.Гефле, С.М.Лебедев, Ю.П.Похолков. Частотные спектры комплексной диэлектрической проницаемости композиционных диэлектриков на основе поливинилхлорида. Математика и механика. Физика. Известия Томского политехнического университета. 2007. Т. 310. №1, с.87-91.
3. В.А.Гончаров, В.И.Архипов. Определение концентрационной зависимости диэлектрической проницаемости водного раствора ацетона по коэффициенту передачи четырёхполюсника. Вестник Казанского Технологического Университета. 2012, Т.15, №14, с.60-63.
4. Ахадов Я.Ю. Диэлектрические параметры чистых жидкостей. М.: МАИ, 1999. 854 с.
5. Золотаревский А.И., Лущин С.П. Исследование спектральной зависимости диэлектрической проницаемости некоторых полярных диэлектриков в диапазоне низких частот. Электротехника и Энергетика 2017. №1, с.6-10.
6. Годжаев Э.М., Алиева Ш.В., Салимова В.В. Фазовый анализ и оптические функции композитов на базе полиэтилена низкой плотности с наполнителями биологического происхождения. Вестник МГТУ им. Н.Э.Баумана. Серия Машиностроение, Москва, 2017. №3(114), с. 90-101.
7. Səlimova, V.V. ASPE + xəcm % Bl pulcuq biokompozitlərinin dielektrik nüfuzluqlarına əsasən optik funksiyalarının hesablanması. Gənc tədqiqatçıların I elmi-praktiki konfransının materialları. Bakı, 05-06 May, - 2017, s.49-50.
8. Əliyeva Ş.V., V.V.Səlimova, S.İ.Məmmədova, G.S.Cəfərova. Biokompozitlərin dielektrik nüfuzluqlarının eksperimental qiymətlərinə əsasən optik funksiyalarının hesablanması. AzTU, Elmi əsərlər, Bakı, 2016. №2, s.51-58.

UOT: 539.12-17**PACS:12.60. - i, 14.70. Bh, 14.70. Dj, 14.80. Da**

THE DECAY OF POLARIZED CHARGINO (NEUTRALINO) INTO HIGGS BOSONS

ABDULLAYEV S. K. , OMAROVA E. SH.

Baku State University

Baku / AZERBAIJAN

*sabdullayev@bsu.edu.az, emiliya.abdullayeva@inbox.ru***ABSTRACT**

In the framework of the Minimal Supersymmetric Standard Model, the decays of the heavy chargino (neutralino) into lightest chargino (neutralino) and the Higgs bosons are considered : $\tilde{\chi}_2^\mp \Rightarrow \tilde{\chi}_1^\mp + h(H; A)$, $\tilde{\chi}_{3,4}^0 \Rightarrow \tilde{\chi}_{1,2}^0 + h(H; A)$, $\tilde{\chi}_2^\mp \Rightarrow \tilde{\chi}_1^0 + H^\mp$. Taking into account the polarization states of the chargino (neutralino) analytical expressions for the decay width are obtained. The degrees of longitudinal and transverse polarizations of the chargino and neutralino, as well as the asymmetry due to the polarization of the initial chargino (neutralino), were determined. The dependence of these characteristics and the decay width on the chargino (neutralino) mass has been studied.

Keywords: Standard Model, Minimal Supersymmetric Standard Model, chargino, neutralino, Higgs-boson, decay width.

POLYARIZƏ OLUNMUŞ ÇARCİNÖNUN (NEYTRALİNÖNUN) HİQQS BOZONLARA PARÇALANMASI**XÜLASƏ**

Minimal Supersimmetrik Standart Model çərçivəsində polyarizə olunmuş ağır carcinonun (neytralinonun) yüngül carcinino (neytralino) ilə Higgs bozona parçalanması proseslərinə baxılmışdır : $\tilde{\chi}_2^\mp \Rightarrow \tilde{\chi}_1^\mp + h(H; A)$, $\tilde{\chi}_{3,4}^0 \Rightarrow \tilde{\chi}_{1,2}^0 + h(H; A)$, $\tilde{\chi}_2^\mp \Rightarrow \tilde{\chi}_1^0 + H^\mp$. Carcinonun (neytralinonun) polyarizasiya halları nəzərə almaqla parçalanma enləri üçün analitik ifadələr alınmışdır. Carcino və neytralino uzununa və eninə polyarizə olunma dərəceləri, həmçinin də başlangıç carcinonun (neytralinonun) uzununa və eninə spin asimetriyaları təyin edilmişdir. Həmin xarakteristikaların və proseslərin parçalanma enlərinin carcinonun və neytralinonun kütlələrindən asılılıqları ətraflı öyrənilmişdir.

Açar sözlər: Standart Model, Minimal Supersimmetrik Standart Model, carcinino, neytralino, Higgs bozon, parçalanma eni.

РАСПАД ПОЛЯРИЗОВАННЫХ ЧАРДЖИНО (НЕЙТРАЛИНО) В ХИГС – БОЗОНЫ**РЕЗЮМЕ**

В рамках Минимальной Суперсимметричной Стандартной Модели рассмотрены распады тяжелого чарджино (нейтралино) в легкое чарджино (нейтралино) и Хигс бозон : $\tilde{\chi}_2^\mp \Rightarrow \tilde{\chi}_1^\mp + h(H; A)$, $\tilde{\chi}_{3,4}^0 \Rightarrow \tilde{\chi}_{1,2}^0 + h(H; A)$, $\tilde{\chi}_2^\mp \Rightarrow \tilde{\chi}_1^0 + H^\mp$. С учетом поляризационных состояний чарджино (нейтралино) получены аналитические выражения для ширины распадов. Определены степени продольных и поперечных поляризаций чарджино и нейтралино, а также асимметрию, обусловленной поляризацией начального чарджино (нейтралино). Изучена зависимость этих характеристик и ширины распадов от массы чарджино (нейтралино).

Ключевые слова: Минимальная Суперсимметричная Стандартная Модель, Хигс бозон, чарджино, нейтралино, ширина распада.

1. Intorduction

With the discovery of the Higgs boson H_{SM} at the Large Hadron Collider (LHC) by the ATLAS and CMS collaborations in 2012 [1,2] (see also reviews [3-6]), a new era in an elementary

particle physics began. The mechanism of generation of masses of fundamental particles - the mechanism of spontaneous breaking of the local gauge symmetry of Braut – Englert – Higgs [7,8] was experimentally confirmed. Thus, the Standard Model (SM) of fundamental interactions received its logical conclusion and acquired the status of a standard theory. The SM based on the local gauge symmetry group $SU_C(3) \times SU_L(2) \times U_Y(1)$ describes the strong, electromagnetic and weak interactions between quarks and leptons. According to the SM, the carriers of strong, electromagnetic and weak interactions are gluons, a photon, charged W^\pm - boson and neutral Z - bosons. Now a fourth, the Yukawa interaction, carried by the Higgs boson, has been added to them. Based on SM, Feynman diagrams of various processes can be calculated and compared with the corresponding experimental results. The agreement between SM and experiment is strikingly good.

Despite the success of SM, this theory has its own difficulties. The main difficulties are associated with the fact that this theory describes a lot, but does not allow it to be derived from deeper principles. One mysterious feature of the SM is a very large spread in the masses of fundamental fermions - quarks and leptons. The top - quark $m_t = 173.2$ GeV has the largest mass, and the electron $m_e = 5 \cdot 10^{-4}$ GeV has the smallest mass. The masses of the top quark and the electron differ by hundreds of thousands of times. Thus, the masses of fundamental fermions are scattered over a very wide range. This situation looks abnormal. Within the framework of the Standard Model, such a mass spread does not receive a satisfactory explanation. However, in non-standard theories, similar mass spreads can occur.

The second difficulty of the SM is related to the renormalization of the mass of the standard Higgs boson. For all SM particles, the mass renormalization works well, however, in the case of the Higgs boson, a problem arises: the vacuum has a strong effect on the mass of the Higgs boson, its mass increases by a factor of trillions and such a particle can no longer play the role of the Higgs boson. There is no restraining factor inside the SM that stops the growth of the Higgs boson mass due to virtual particles. Here such a way out of the difficult situation is possible. If there are some particles in nature that are absent in the SM, then in virtual form they can compensate for the effect on the Higgs boson mass. The most important thing here is that in models outside the SM, such compensation itself arises from the construction of the theory.

The absence of dark matter particles in the SM is also one of the difficulties of this theory. In astrophysics, it is believed that in the Universe, in addition to particles of ordinary matter, there are also particles of dark matter. We do not see them, they practically do not interact with ordinary matter and radiation. There is not a single particle in the SM that is suitable for this role. In theories outside the SM, there are such particles as neutralino, sneutrino, gluino, gravitino, which can be candidates for dark matter particles.

All the above facts, as well as other reasons, indicate the need to go beyond the framework of the SM. What opportunities are there for expanding the SM? The focus is on the two-doublet Higgs model (2HDM) [9,10] and the Minimal Supersymmetric Standard Model (MSSM) [11-13].

In the MSSM, two scalar field doublets with hypercharges -1 and $+1$ are introduced:

$$\varphi_1 = \begin{pmatrix} H_1^0 \\ H_1^- \end{pmatrix}, \quad \varphi_2 = \begin{pmatrix} H_2^+ \\ H_2^0 \end{pmatrix}.$$

In order to obtain the physical fields of Higgs bosons, the scalar fields φ_1 and φ_2 are represented in the form

$$\varphi_1 = \frac{1}{\sqrt{2}} \begin{pmatrix} v_1 + H_1^0 + iP_1^0 \\ H_1^- \end{pmatrix}, \varphi_2 = \frac{1}{\sqrt{2}} \begin{pmatrix} H_2^+ \\ v_2 + H_2^0 + iP_2^0 \end{pmatrix},$$

where H_1^0, P_1^0, H_2^0 and P_2^0 are the fields describing the excitations of the system with respect to the vacuum states $\langle \varphi_1 \rangle = \frac{1}{\sqrt{2}} v_1$ and $\langle \varphi_2 \rangle = \frac{1}{\sqrt{2}} v_2$.

CP-even Higgs bosons H and h are obtained by mixing the H_1^0 and H_2^0 fields (mixing angle α):

$$\begin{pmatrix} H \\ h \end{pmatrix} = \begin{pmatrix} \cos \alpha & \sin \alpha \\ -\sin \alpha & \cos \alpha \end{pmatrix} \begin{pmatrix} H_1^0 \\ H_2^0 \end{pmatrix}.$$

Similarly, by mixing the fields P_1^0 and P_2^0 , (H_1^\pm and H_2^\pm), a Goldstone boson G^0 and a CP-odd Higgs boson A are obtained (Goldstone bosons G^\pm and charged Higgs bosons H^\pm):

$$\begin{pmatrix} G^0 \\ A \end{pmatrix} = \begin{pmatrix} \cos \beta & \sin \beta \\ -\sin \beta & \cos \beta \end{pmatrix} \begin{pmatrix} P_1^0 \\ P_2^0 \end{pmatrix}, \quad \begin{pmatrix} G^\pm \\ H^\pm \end{pmatrix} = \begin{pmatrix} \cos \beta & \sin \beta \\ -\sin \beta & \cos \beta \end{pmatrix} \begin{pmatrix} H_1^\pm \\ H_2^\pm \end{pmatrix}.$$

here β is a field mixing angle.

Thus, there are five Higgs bosons in the MSSM: CP-even H - and h -bosons, CP-odd A -boson, and charged H^+ - and H^- -bosons.

The Higgs sector of the MSSM are characterized by parameters M_h, M_H, M_A, M_{H^\pm} , α and β , of them, the parameters M_A and $\tan \beta = \frac{v_2}{v_1}$ are considered free. The rest of the parameters are expressed through them:

$$M_{h(H)}^2 = \frac{1}{2} \left[M_A^2 + M_Z^2 \mp \sqrt{(M_A^2 + M_Z^2)^2 - 4M_A^2 M_Z^2 \cos^2 2\beta} \right],$$

$$M_{H^\pm}^2 = M_A^2 + M_W^2,$$

$$\tan 2\alpha = \tan 2\beta \cdot \frac{M_A^2 + M_Z^2}{M_A^2 - M_Z^2}, \quad \left(-\frac{\pi}{2} \leq \alpha < 0 \right).$$

Where M_W and M_Z is the masses of the gauge W^\pm - and Z -bosons.

In the MSSM there are two charged charginos $\tilde{\chi}_i^\pm (i=1,2)$ and four neutralinos $\tilde{\chi}_j^0 (j=1,2,3,4)$. Chargino is the result of mixing calibrino \tilde{W}^\pm and higgsino $\tilde{H}_1^+, \tilde{H}_2^-$, while neutralino is superpositions of photino $\tilde{\gamma}$, zino \tilde{Z} , and higgsino $\tilde{H}_1^0, \tilde{H}_2^0$.

Higgs - bosons H , h and A can decay into both ordinary particles and supersymmetric (SUSY) particles (chargino, neutralino, sfermions) [11, 14-25]. If the mass of the Higgs boson $H_k (k=1,2,3,4)$ for the Higgs bosons, H , h , A and H^\pm) is greater than the sums of the masses of the chargino (neutralino) pairs $M_{H_k} > m_{\tilde{\chi}_i} + m_{\tilde{\chi}_j}$, then the Higgs boson decay into a chargino

(neutralino) pair is energetically possible $H_k \Rightarrow \tilde{\chi}_i + \tilde{\chi}_j$. However, if $M_{H_k} < m_{\tilde{\chi}_i} + m_{\tilde{\chi}_j}$, then the decay is not allowed $H_k \Rightarrow \tilde{\chi}_i + \tilde{\chi}_j$. Under this condition, the decay of a heavier chargino (neutralino) into a lightest chargino (neutralino) and a Higgs boson is possible:

$$\tilde{\chi}_2^\mp \Rightarrow \tilde{\chi}_1^\pm + H_k, \quad (1)$$

$$\tilde{\chi}_{3,4}^0 \Rightarrow \tilde{\chi}_{1,2}^0 + H_k, \quad (2)$$

$$\tilde{\chi}_2^\pm \Rightarrow \tilde{\chi}_1^0 + H^\pm. \quad (3)$$

In this work, taking into account the polarization states of the initial and final chargino and neutralino, an analytical expression for the decay width (1) - (3) is obtained, the degrees of longitudinal and transverse polarization of the chargino (neutralino) and the dependence of these characteristics, as well as the decay width, on the chargino (neutralino) mass are determined.

2. Masses and constants of interaction chargino and neutralino

Chargino mass matrix depends on mass parameters of vino M_2 and Higgsino μ , as well as on the parameter $\tan \beta$ [15, 26]:

$$M_{\tilde{\chi}^\pm} = \begin{pmatrix} M_2 & \sqrt{2}M_W \sin \beta \\ \sqrt{2}M_W \cos \beta & \mu \end{pmatrix}. \quad (4)$$

This matrice is diagonalized by two real U and V matrices:

$$UM_{\tilde{\chi}^\pm}V^{-1} \Rightarrow U = R_- \text{ and } V = \begin{cases} R_+ & \text{if } \det M_{\tilde{\chi}^\pm} > 0, \\ \sigma_3 R_+ & \text{if } \det M_{\tilde{\chi}^\pm} < 0, \end{cases}$$

where σ_3 is a Pauli matrice which making the chargino mass positive, R_\pm is a rotation matrices with angles θ_\pm

$$R_\pm = \begin{pmatrix} \cos \theta_\pm & \sin \theta_\pm \\ -\sin \theta_\pm & \cos \theta_\pm \end{pmatrix},$$

where

$$\tan 2\theta_+ = \frac{2\sqrt{2}M_W(M_2 \sin \beta + \mu \cos \beta)}{M_2^2 - \mu^2 + 2M_W^2 \cos \beta}, \quad \tan 2\theta_- = \frac{2\sqrt{2}M_W(M_2 \cos \beta + \mu \sin \beta)}{M_2^2 - \mu^2 - 2M_W^2 \cos \beta}.$$

This leads to $\tilde{\chi}_1^\mp$ and $\tilde{\chi}_2^\mp$ charginos with masses

$$m_{\tilde{\chi}_{1,2}^\pm}^2 = \frac{1}{2} \left[M_2^2 + \mu^2 + 2M_W^2 \mp \sqrt{(M_2^2 - \mu^2)^2 + 4M_W^2(M_W^2 \cos^2 2\beta + M_2^2 + \mu^2 + 2M_2 \mu \sin 2\beta)} \right]. \quad (5)$$

At the limit $|\mu| \gg M_2, M_W$, the masses of the two charginos are equal:

$$m_{\tilde{\chi}_1^\pm} \approx M_2 - \frac{M_W^2}{\mu^2} (M_2 + \mu \sin 2\beta), \quad (6)$$

$$m_{\tilde{\chi}_2^\pm} \approx |\mu| + \frac{M_W^2}{\mu^2} \varepsilon_\mu (M_2 \sin 2\beta + \mu),$$

where ε_μ defines the sign of the parameter μ : $\varepsilon_\mu = \mu/|\mu|$.

At $|\mu| \rightarrow \infty$, a lightest chargino corresponds to the state of vino with a mass $m_{\tilde{\chi}_1^\pm} \cong M_2$, and a heavy chargino to a state of a Higgsino with a mass $m_{\tilde{\chi}_2^\pm} \cong |\mu|$.

In the case of neutralino, the mass matrix depends on the same parameters M_1, μ and $\tan \beta$, as well as on the additional bino mass parameter M_2 (θ_W is the Weinberg angle) [15,17]:

$$M_{\tilde{\chi}^0} = \begin{pmatrix} M_1 & 0 & -M_Z \sin \theta_W \cos \beta & M_Z \sin \theta_W \sin \beta \\ 0 & M_2 & M_Z \cos \theta_W \cos \beta & -M_Z \cos \theta_W \sin \beta \\ -M_Z \sin \theta_W \cos \beta & M_Z \cos \theta_W \cos \beta & 0 & -\mu \\ M_Z \sin \theta_W \sin \beta & -M_Z \cos \theta_W \sin \beta & \mu & 0 \end{pmatrix}. \quad (7)$$

This matrix can be diagonalized with one real matrix Z [15,17]. In the limit of large values of the $|\mu|(|\mu| >> M_{1,2} >> M_Z)$ parameter, the neutralino masses are determined by the expressions [11]:

$$\begin{aligned} m_{\tilde{\chi}_1^0} &\cong M_1 - \frac{M_Z^2}{\mu^2} (M_1 + \mu \sin 2\beta) \sin^2 \theta_W, \\ m_{\tilde{\chi}_2^0} &\cong M_2 - \frac{M_Z^2}{\mu^2} (M_2 + \mu \sin 2\beta) \cos^2 \theta_W, \\ m_{\tilde{\chi}_3^0} &\cong |\mu| + \frac{M_Z^2}{2\mu^2} \varepsilon_\mu (1 - \sin 2\beta)(\mu + M_2 \sin^2 \theta_W + M_1 \cos^2 \theta_W), \\ m_{\tilde{\chi}_4^0} &\cong |\mu| + \frac{M_Z^2}{2\mu^2} \varepsilon_\mu (1 + \sin 2\beta)(\mu - M_2 \sin^2 \theta_W - M_1 \cos^2 \theta_W). \end{aligned} \quad (8)$$

Again at $|\mu| \rightarrow \infty$, two neutralinos correspond to the gaugino state with masses $m_{\tilde{\chi}_1^0} \cong M_1$, $m_{\tilde{\chi}_2^0} \cong M_2$, the rest of the neutralinos correspond to a purely Higgsino state with $m_{\tilde{\chi}_3^0} \cong m_{\tilde{\chi}_4^0} \cong |\mu|$ masses.

The matrix elements of Z_{ij} ($i, j = 1, 2, 3, 4$) diagonalizing the mass matrix of neutralino are determined by the expressions [15,17]:

$$\begin{aligned} Z_{i1} &= \left[1 + \left(\frac{Z_{i2}}{Z_{i1}} \right)^2 + \left(\frac{Z_{i3}}{Z_{i1}} \right)^2 + \left(\frac{Z_{i4}}{Z_{i1}} \right)^2 \right]^{-\frac{1}{2}}, \\ \frac{Z_{i2}}{Z_{i1}} &= -\frac{1}{\tan^2 \theta_W} \cdot \frac{M_1 - \varepsilon_i m_{\tilde{\chi}_i^0}}{M_2 - \varepsilon_i m_{\tilde{\chi}_i^0}}, \\ \frac{Z_{i3}}{Z_{i1}} &= \frac{\mu(M_1 - \varepsilon_i m_{\tilde{\chi}_i^0})(M_2 - \varepsilon_i m_{\tilde{\chi}_i^0}) - 0.5 M_Z^2 \sin 2\beta [(M_1 - M_2) \cos^2 \theta_W + M_2 - \varepsilon_i m_{\tilde{\chi}_i^0}]}{M_Z (M_2 - \varepsilon_i m_{\tilde{\chi}_i^0}) \sin \theta_W [\mu \cos \beta + \varepsilon_i m_{\tilde{\chi}_i^0} \sin \beta]}, \\ \frac{Z_{i4}}{Z_{i1}} &= \frac{-\varepsilon_i m_{\tilde{\chi}_i^0} (M_1 - \varepsilon_i m_{\tilde{\chi}_i^0})(M_2 - \varepsilon_i m_{\tilde{\chi}_i^0}) - M_Z^2 \cos^2 \beta [(M_1 - M_2) \cos^2 \theta_W + M_2 - \varepsilon_i m_{\tilde{\chi}_i^0}]}{M_Z (M_2 - \varepsilon_i m_{\tilde{\chi}_i^0}) \sin \theta_W [\mu \cos \beta + \varepsilon_i m_{\tilde{\chi}_i^0} \sin \beta]}. \end{aligned} \quad (9)$$

Here $\varepsilon_1 = \varepsilon_2 = 1$, $\varepsilon_4 = -\varepsilon_3 = \varepsilon_\mu$.

The coupling constants of the Higgs bosons H_k ($k = 1, 2, 3, 4$ for H , h , A and H^\pm bosons) with a pair of charginos (neutralino) and chargino-neutralino are determined by the expressions [11, 18]:

$$\begin{aligned} g_{ijk}^L &= \frac{1}{\sqrt{2}}[V_{jl}U_{i2}e_k - V_{j2}U_{il}d_k], \\ g_{H_k\tilde{\chi}_i^-\tilde{\chi}_j^+}^{L,R} &= g_{ijk}^{L,R} \Rightarrow \\ g_{ijk}^R &= \frac{1}{\sqrt{2}}[V_{il}U_{j2}e_k - V_{i2}U_{jl}d_k]\varepsilon_k, \end{aligned} \quad (10)$$

$$\begin{aligned} g_{H_k\tilde{\chi}_i^0\tilde{\chi}_j^0}^{L,R} &= g_{ijk}^{L,R} \Rightarrow \\ g_{ijk}^R &= \frac{1}{2}(Z_{j2} - tg\theta_W Z_{j1})(Z_{i3}e_k + Z_{i4}d_k)\varepsilon_k + i \rightarrow j, \\ g_{ijk}^L &= \cos\beta[V_{il}Z_{j4} + \frac{1}{\sqrt{2}}V_{i2}(Z_{j2} + tg\theta_W Z_{j1})], \end{aligned} \quad (11)$$

$$\begin{aligned} g_{H_k\tilde{\chi}_i^-\tilde{\chi}_j^0}^{L,R} &= g_{ijk}^{L,R} \Rightarrow \\ g_{ijk}^R &= \sin\beta[U_{il}Z_{j3} - \frac{1}{\sqrt{2}}U_{i2}(Z_{j2} + tg\theta_W Z_{j1})], \end{aligned} \quad (12)$$

$\varepsilon_1 = \varepsilon_2 = -\varepsilon_3 = 1$ is coefficient, e_k and d_k are equal:

$$\begin{aligned} e_1 &= \cos\alpha, e_2 = -\sin\alpha, e_3 = -\sin\beta, \\ d_1 &= -\sin\alpha, d_2 = -\cos\alpha, d_3 = \cos\beta. \end{aligned}$$

3. Amplitudes and widths of decays (1) – (3)

The decay process of heavy chargino (neutralino) into lightest chargino (neutralino) and Higgs boson corresponds to the Feynman diagram shown in Fig. 2. Here p , p_1 and p_2 are 4-momentums of the initial chargino (neutralino), final chargino (neutralino), and Higgs boson; s and s_1 are the 4-polarization vectors of the initial and final chargino (neutralino).

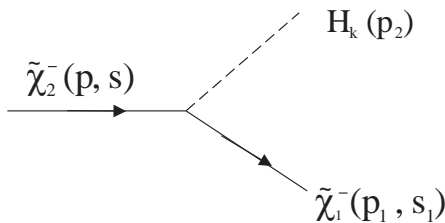


Fig. 1. Feynman diagram for decay $\tilde{\chi}_2^- \Rightarrow \tilde{\chi}_1^- H_k$

The amplitude of process can be represented as:

$$M_{i \rightarrow f} = ig[g_{ijk}^L \bar{u}(p_1, s_1) P_L u(p, s) + g_{ijk}^R \bar{u}(p_1, s_1) P_R u(p, s)], \quad (13)$$

where g is a constant that determines the mass of W^\pm -boson in MSSM: $M_W^2 = \frac{1}{2} g^2 (v_1^2 + v_2^2)$;

$P_{L,R} = \frac{(1 \pm \gamma_5)}{2}$ is chirality matrices; g_{ijk}^L and g_{ijk}^R are the coupling constants of the Higgs boson H_k with a pair of charginos (neutralino) (they are determined by expressions (10) - (12)):

For the square of the matrix element (13), the following expression is found in a standard way:

$$|M_{i \rightarrow f}|^2 = \frac{g^2}{2} \left\{ [(g_{ijk}^L)^2 + (g_{ijk}^R)^2] [(p \cdot p_1) - m_{\tilde{\chi}_i} m_{\tilde{\chi}_j} (s \cdot s_1)] + [(g_{ijk}^L)^2 - (g_{ijk}^R)^2] [m_{\tilde{\chi}_i} (p \cdot s_1) - m_{\tilde{\chi}_j} (p_1 \cdot s)] + 2g_{ijk}^L g_{ijk}^R [m_{\tilde{\chi}_i} m_{\tilde{\chi}_j} + (p \cdot s_1)(p_1 \cdot s) - (p \cdot p_1)(s \cdot s_1)] \right\}. \quad (14)$$

The decay width of processes (1) - (3) in the rest system of the initial chargino (neutralino) is determined by the formula

$$d\Gamma = \frac{1}{2m_{\tilde{\chi}_i^-}} |M_{i \rightarrow f}|^2 \cdot d\Phi, \quad (15)$$

where

$$d\Phi = (2\pi)^4 \delta(p - p_1 - p_2) \frac{d\vec{p}_1}{(2\pi)^3 \cdot 2E_1} \cdot \frac{d\vec{p}_2}{(2\pi)^3 \cdot 2E_2} \quad (16)$$

is a phase volume; E_1 and E_2 are the energies of the final chargino (neutralino) and Higgs boson, \vec{p}_1 and \vec{p}_2 are their momentums.

After integrating over the momenta of the chargino (neutralino) and over the energy of the Higgs boson, for the decay width $\tilde{\chi}_2^\mp \rightarrow \tilde{\chi}_1^\mp + H_k$ ($\tilde{\chi}_{3,4}^0 \rightarrow \tilde{\chi}_{1,2}^0 + H_k$, $\tilde{\chi}_2^\mp \rightarrow \tilde{\chi}_1^0 + H^\mp$) in the rest system of the initial chargino (neutralino), we obtain the formula:

$$\begin{aligned} \frac{d\Gamma(\tilde{\xi}, \tilde{\xi}_1)}{d\Omega} = & \frac{G_F M_W^2}{32\sqrt{2}\pi^2} m_{\chi_i} \sqrt{\lambda(r_{\chi_j}, r_{H_k})} \left\{ [(g_{ijk}^L)^2 + (g_{ijk}^R)^2] [(1 + r_{\chi_j} - r_{H_k})(1 + (\vec{n}\vec{\xi})(\vec{n}\vec{\xi}_1))] + \right. \\ & + 2\sqrt{r_{\chi_j}} ((\vec{\xi}\vec{\xi}_1) - (\vec{n}\vec{\xi})(\vec{n}\vec{\xi}_1)) - [(g_{ijk}^L)^2 - (g_{ijk}^R)^2] \sqrt{\lambda(r_{\chi_j}, r_{H_k})} [(\vec{n}\vec{\xi}) + (\vec{n}\vec{\xi}_1)] + \\ & \left. + 2g_{ijk}^L g_{ijk}^R [2\sqrt{r_{\chi_j}} (1 + (\vec{n}\vec{\xi})(\vec{n}\vec{\xi}_1)) + (1 + r_{\chi_j} - r_{H_k})((\vec{\xi}\vec{\xi}_1) - (\vec{n}\vec{\xi})(\vec{n}\vec{\xi}_1))] \right\}. \end{aligned} \quad (17)$$

Here G_F is the Fermi constant of weak interactions; \vec{n} is a unit vector in the direction on the Higgs boson momentum; $\vec{\xi}$ and $\vec{\xi}_1$ are unit vectors characterizing the polarizations of the charginos and neutralinos in their rest systems;

$$\lambda(r_{\chi_j}, r_{H_k}) = (1 - r_{\chi_j} - r_{H_k})^2 - 4r_{\chi_j} r_{H_k} \quad (18)$$

is a kinematic function of two-particle phase volume, $d\Omega = d(\cos\theta)d\phi$ is a solid angle of departure of the Higgs boson; through r_{χ_j} and r_{H_k} are introduced notation

$$r_{\chi_j} = \left(\frac{m_{\chi_j}}{m_{\chi_i}} \right)^2, \quad r_{H_k} = \left(\frac{M_{H_k}}{m_{\chi_i}} \right)^2,$$

where m_{χ_i} and m_{χ_j} are a mass of heavy and lightest chargino (neutralino).

We direct the Z axis along the unit spin vector of the initial chargino (neutralino) $\vec{\xi}$ (see Fig. 2), then the unit vector \vec{n} will have projections

$$\vec{n} = (\sin \theta \cos \varphi, \sin \theta \sin \varphi, \cos \theta),$$

where θ and φ are the polar and azimuthal angles of departure of the Higgs boson. First, suppose that the final chargino (neutralino) is longitudinally polarized. Moreover, we have:

$$(\vec{n} \vec{\xi}) = \xi \cos \theta, \quad (\vec{n} \vec{\xi}_1) = -\lambda, \quad (\vec{\xi} \vec{\xi}_1) = -\xi \lambda \cos \theta,$$

where λ is the spirality of the final chargino (neutralino).

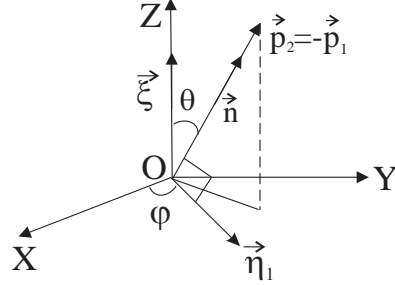


Fig. 2. Selected coordinate system

In this case, for the decay width of the processes (1) - (3) we have the expression (integrated over the azimuthal angle φ) :

$$\begin{aligned} \frac{d\Gamma(\xi, \lambda)}{d(\cos \theta)} &= \frac{G_F M_W^2}{16\sqrt{2}\pi} m_{\chi_i} \sqrt{\lambda(r_{\chi_j}, r_{H_k})} \left\{ [(g_{ijk}^L)^2 + (g_{ijk}^R)^2] (1 + r_{\chi_j} - r_{H_k}) + \right. \\ &+ 4 g_{ijk}^L g_{ijk}^R \sqrt{r_{\chi_j}} [(1 - \lambda \xi \cos \theta) + [(g_{ijk}^L)^2 - (g_{ijk}^R)^2] \sqrt{\lambda(r_{\chi_j}, r_{H_k})}] (\lambda - \xi \cos \theta) \Big\}. \end{aligned} \quad (19)$$

If only the initial chargino (neutralino) is polarized, then the decay width is expressed by the formula :

$$\frac{d\Gamma(\xi)}{d(\cos \theta)} = \frac{d\Gamma_0}{d(\cos \theta)} (1 + \xi A_{II}). \quad (20)$$

Here

$$\frac{d\Gamma_0}{d(\cos \theta)} = \frac{G_F M_W^2}{8\sqrt{2}\pi} m_{\chi_i} \sqrt{\lambda(r_{\chi_j}, r_{H_k})} \left\{ [(g_{ijk}^L)^2 + (g_{ijk}^R)^2] (1 + r_{\chi_j} - r_{H_k}) + 4 g_{ijk}^L g_{ijk}^R \sqrt{r_{\chi_j}} \right\} \quad (21)$$

is decay width in case of unpolarized particles, and

$$A_{II} = \frac{[(g_{ijk}^L)^2 - (g_{ijk}^R)^2] \sqrt{\lambda(r_{\chi_j}, r_{H_k})} \cos \theta}{[(g_{ijk}^L)^2 + (g_{ijk}^R)^2] (1 + r_{\chi_j} - r_{H_k}) + 4 g_{ijk}^L g_{ijk}^R \sqrt{r_{\chi_j}}}. \quad (22)$$

is longitudinal spin asymmetry due to polarization of the initial chargino (neutralino).

If we were interested in the dependence of the decay width on the spin direction of the final chargino (neutralino), we would get the following expression for the decay width, integrated over the particle emission angles :

$$\Gamma(\lambda) = \frac{1}{2} \Gamma_0 (1 + \lambda P_{II}) , \quad (23)$$

where

$$\Gamma_0 = \frac{G_F M_W^2}{4\sqrt{2}\pi} m_{\tilde{\chi}_2^-} \sqrt{\lambda(r_{\chi_j}, r_{H_k})} \{ [(g_{ijk}^L)^2 + (g_{ijk}^R)^2] (1 + r_{\chi_j} - r_{H_k}) + 4 g_{ijk}^L g_{ijk}^R \sqrt{r_{\chi_j}} \} \quad (24)$$

is a total decay width, and P_{II} is the degree of longitudinal polarization of the chargino (neutralino) :

$$P_{II} = \frac{[(g_{ijk}^L)^2 - (g_{ijk}^R)^2] \sqrt{\lambda(r_{\chi_j}, r_{H_k})}}{[(g_{ijk}^L)^2 + (g_{ijk}^R)^2] (1 + r_{\chi_j} - r_{H_k}) + 4 g_{ijk}^L g_{ijk}^R \sqrt{r_{\chi_j}}} . \quad (25)$$

Now suppose that the final chargino (neutralino) is transversely polarized in the plane of Higgs boson - chargino (neutralino) production. Moreover, we have:

$$(\vec{n} \vec{\xi}) = (\vec{n} \vec{\eta}) = 0 , \quad (\vec{n} \vec{\xi}_1) = (\vec{n} \vec{\eta}_1) = 0 , \quad (\vec{\xi} \vec{\xi}_1) = (\vec{\eta} \vec{\eta}_1) = 0 ,$$

As a result of these relations, the decay width of the processes (1) - (3) is insensitive to the transverse polarizations of the initial and final chargino (neutralino). Here $\vec{\eta}$ and $\vec{\eta}_1$ are the unit vectors of the transverse polarizations of the chargino (neutralino).

If the final chargino (neutralino) is transversely polarized in the plane of Higgs boson - chargino (neutralino) production, then

$$(\vec{n} \vec{\xi}_1) = (\vec{n} \vec{\eta}_1) = 0 , \quad (\vec{n} \vec{\xi}) = (\vec{n} \vec{\eta}) = -\eta \sin \theta , \quad (\vec{\xi} \vec{\xi}_1) = (\vec{\eta} \vec{\eta}_1) = -\eta \eta_1 \sin \theta ,$$

and for the differential decay width of the processes (1) - (3) we obtain the following expression :

$$\frac{d\Gamma(\eta, \eta_1)}{d(\cos \theta)} = \frac{1}{2} \cdot \frac{d\Gamma_0}{d(\cos \theta)} (1 + A_{\perp} \eta + P_{\perp} \eta \eta_1) . \quad (26)$$

Here

$$A_{\perp} = \frac{2 \sin \theta [(g_{ijk}^L)^2 - (g_{ijk}^R)^2] \sqrt{\lambda(r_{\chi_j}, r_{H_k})}}{[(g_{ijk}^L)^2 + (g_{ijk}^R)^2] (1 + r_{\chi_j} - r_{H_k}) + 4 g_{ijk}^L g_{ijk}^R \sqrt{r_{\chi_j}}} \quad (27)$$

is a transverse spin asymmetry due to the transverse polarization of the initial chargino (neutralino) and P_{\perp} is the degree of transverse polarization of the final chargino (neutralino) during the decay of the transversely polarized chargino (neutralino) :

$$P_{\perp} = -2 \sin \theta \cdot \frac{[(g_{ijk}^L)^2 + (g_{ijk}^R)^2] \sqrt{r_{\chi_j}} + g_{ijk}^L g_{ijk}^R (1 + r_{\chi_j} - r_{H_k})}{[(g_{ijk}^L)^2 + (g_{ijk}^R)^2] (1 + r_{\chi_j} - r_{H_k}) + 4 g_{ijk}^L g_{ijk}^R \sqrt{r_{\chi_j}}} . \quad (28)$$

4. Analysis of the obtained results

Let's make estimates the A_{II} and A_{\perp} asymmetries, the degrees of longitudinal P_{II} and P_{\perp} the transverse polarizations of the chargino (neutralino), and the decay widths $\tilde{\chi}_2^- \rightarrow \tilde{\chi}_1^- + h$ ($\tilde{\chi}_{3,4}^0 \rightarrow \tilde{\chi}_{1,2}^0 + h$, $\tilde{\chi}_2^{\mp} \rightarrow \tilde{\chi}_1^0 + H^{\mp}$), where h is the Higgs boson with the minimal mass.

Figure 3 shows the dependence of the longitudinal spin asymmetry A_{II} on the chargino mass in $\tilde{\chi}_2^- \rightarrow \tilde{\chi}_1^- + h$ decay at $\cos\theta=1$, $M_A = 180$ GeV, $\tan\beta = 1$, $M_2 = 150$ GeV. It follows from the figure that the longitudinal spin asymmetry A_{II} in the $\tilde{\chi}_2^- \rightarrow \tilde{\chi}_1^- + h$ decay is negative, with an increase in the chargino mass, the asymmetry increases and reaches a maximum at $m_{\tilde{\chi}_2^-} = 300$ GeV, and a further increase in the chargino mass leads to a decrease in the longitudinal spin asymmetry.

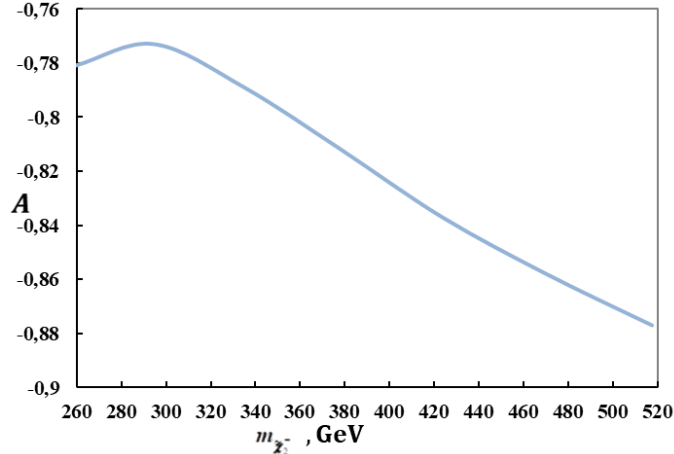


Fig. 3. Dependence of the longitudinal spin asymmetry A_{II} on the chargino mass in the decay $\tilde{\chi}_2^- \Rightarrow \tilde{\chi}_1^- h$

Figure 4 illustrates the dependence of the transverse spin asymmetry A_{\perp} on the chargino mass at an angle $\theta = 120^\circ$ (other parameters are chosen as in Fig. 4). The transverse spin asymmetry, in contrast to the longitudinal spin asymmetry, is positive; with an increase in the chargino mass, it first decreases and reaches a minimum at $m_{\tilde{\chi}_2^-} = 300$ GeV, and then the transverse spin asymmetry monotonically increases with an increase in the chargino mass.

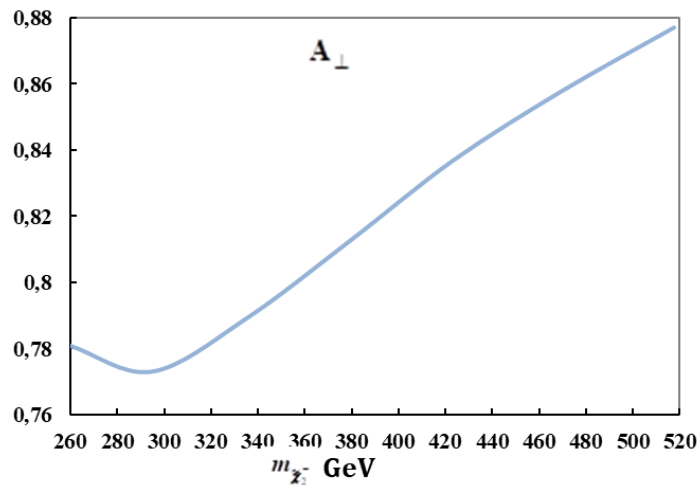


Fig. 4. Dependence of the transverse spin asymmetry A_{\perp} on the chargino mass in the decay $\tilde{\chi}_2^- \Rightarrow \tilde{\chi}_1^- h$

As for the asymmetries A_{II} and A_{\perp} in the neutralino decays $\tilde{\chi}_{3,4}^0 \rightarrow \tilde{\chi}_{1,2}^0 + h$, then due to the equality of the interaction constants $g_{ijk}^L = g_{ijk}^R$, these asymmetries, as well as the degree of longitudinal polarization P_{II} can be vanished.

In fig. 5 shows the dependence of the degree of longitudinal polarization P_{II} on the mass $m_{\tilde{\chi}_2^-}$ for the same parameter values as in Fig. 4. In the $\tilde{\chi}_2^- \Rightarrow \tilde{\chi}_1^- + h$ decay, the degree of longitudinal polarization of the chargino is positive, with an increase in the chargino mass it first decreases, reaches a minimum near $m_{\tilde{\chi}_2^-} = 300$ GeV, and with a further increase in the chargino mass, the degree of its longitudinal polarization increases.

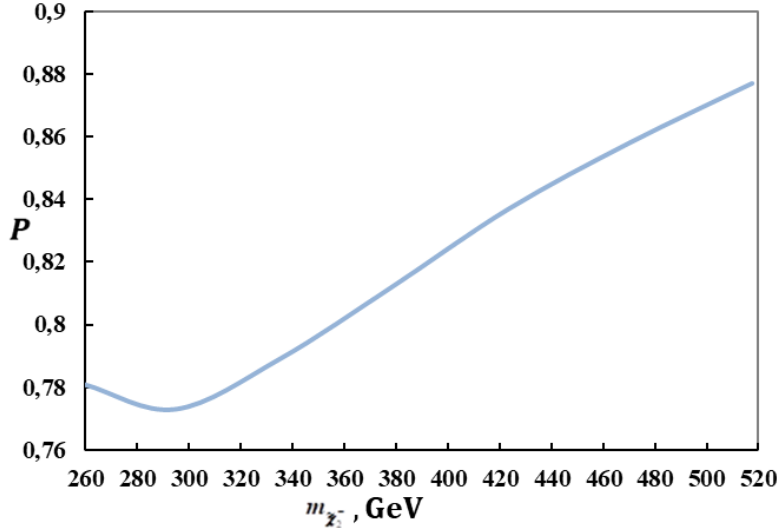


Fig. 5. The degree of longitudinal polarization of the chargino in the $\tilde{\chi}_2^- \Rightarrow \tilde{\chi}_1^- h$ decay as a function of the $m_{\tilde{\chi}_2^-}$ mass

In fig. 6 illustrates the dependence of the degree of transverse polarization of the chargino P_\perp in the $\tilde{\chi}_2^- \Rightarrow \tilde{\chi}_1^- + h$ decay on the $m_{\tilde{\chi}_2^-}$ mass at $\theta = 90^\circ$, $M_A = 180$ GeV, $\tan \beta = 1$, $M_2 = 150$ GeV. It follows from the figure that the degree of transverse polarization is negative, with an increase in the chargino mass, it decreases and reaches a minimum near $m_{\tilde{\chi}_2^-} = 290$ GeV, and a further increase in $m_{\tilde{\chi}_2^-}$ leads to an increase in the degree of transverse polarization.

It should be noted that in the neutralino decays $\tilde{\chi}_{3,4}^0 \rightarrow \tilde{\chi}_{1,2}^0 + h$, the left and right coupling constants of the Higgs boson with a pair of charginos are equal to each other ($g_{ijk}^L = g_{ijk}^R$); therefore, the degree of transverse polarization of the neutralino depends only on the polar angle of the Higgs boson emission θ

$$P_\perp = -\sin \theta. \quad (29)$$

With an increase in the polar angle of the Higgs boson from 0° to 180° , the degree of transverse polarization of the neutralino decreases from zero to -1, then increases again to zero.

Figure 7 shows the dependence of the $\Gamma(\tilde{\chi}_2^- \Rightarrow \tilde{\chi}_1^- h)$ decay width on the chargino mass for the values of the parameters as in Fig. 4-6. With an increase in the mass of the chargino $m_{\tilde{\chi}_2^-}$, the $\tilde{\chi}_2^- \Rightarrow \tilde{\chi}_1^- + h$ decay width increases.

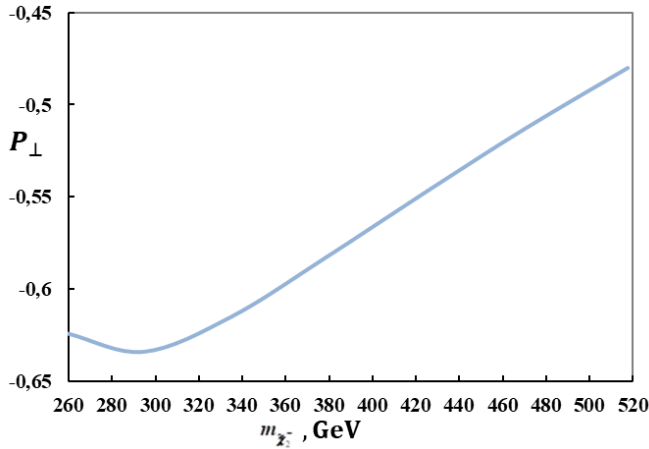


Fig. 6. Dependence of the degree of transverse polarization of the chargino on the mass $m_{\tilde{\chi}_2^-}$

Note that in the $M_A \approx |\mu| \gg M_2$ limit, the partial widths of the decays of a chargino (neutralino) into a light Higgs boson h and a lightest chargino (neutralino) are proportional to the mass parameter $|\mu|$:

$$\begin{aligned} \Gamma(\tilde{\chi}_2^- \Rightarrow \tilde{\chi}_1^- h) &= \frac{G_F M_W^2 |\mu|}{8\sqrt{2}\pi}, \\ \Gamma(\tilde{\chi}_3^0 \Rightarrow \tilde{\chi}_1^0 h) &= \frac{G_F M_W^2 |\mu|}{8\sqrt{2}\pi} \cdot \frac{1}{2} \operatorname{tg}^2 \theta_W (1 - \sin 2\beta), \\ \Gamma(\tilde{\chi}_4^0 \Rightarrow \tilde{\chi}_1^0 h) &= \frac{G_F M_W^2 |\mu|}{8\sqrt{2}\pi} \cdot \frac{1}{2} \operatorname{tg}^2 \theta_W (1 + \sin 2\beta), \\ \Gamma(\tilde{\chi}_3^0 \Rightarrow \tilde{\chi}_2^0 h) &= \frac{G_F M_W^2 |\mu|}{8\sqrt{2}\pi} \cdot \frac{1}{2} (1 - \sin 2\beta), \\ \Gamma(\tilde{\chi}_4^0 \Rightarrow \tilde{\chi}_2^0 h) &= \frac{G_F M_W^2 |\mu|}{8\sqrt{2}\pi} \cdot \frac{1}{2} (1 + \sin 2\beta). \end{aligned} \quad (30)$$

At $|\mu| = 400$ GeV, $\tan \beta = 3$ and $\sin^2 \theta_W = 0.2315$, these partial decay widths are

$$\Gamma(\tilde{\chi}_2^- \Rightarrow \tilde{\chi}_1^- h) = 0.848 \text{ GeV}, \quad \Gamma(\tilde{\chi}_3^0 \Rightarrow \tilde{\chi}_1^0 h) = 0.015 \text{ GeV}, \quad \Gamma(\tilde{\chi}_4^0 \Rightarrow \tilde{\chi}_1^0 h) = 0.062 \text{ GeV},$$

$$\Gamma(\tilde{\chi}_3^0 \Rightarrow \tilde{\chi}_2^0 h) = 0.17 \text{ GeV}, \quad \Gamma(\tilde{\chi}_4^0 \Rightarrow \tilde{\chi}_2^0 h) = 0.678 \text{ GeV}.$$

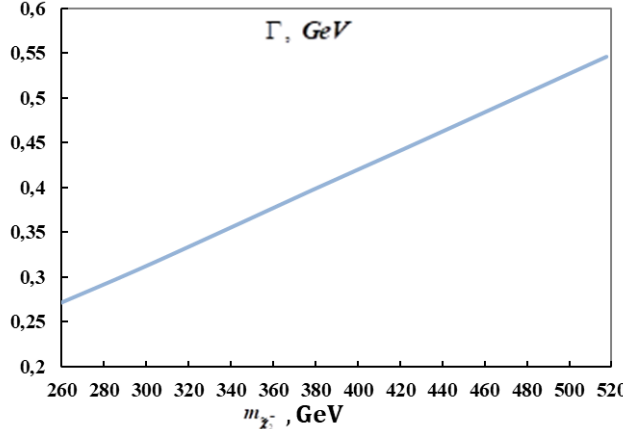


Fig. 7. Decay width $\Gamma(\tilde{\chi}_2^- \Rightarrow \tilde{\chi}_1^- h)$ as a function of $m_{\tilde{\chi}_2^-}$

We have estimated the longitudinal and transverse spin asymmetries A_{II} and A_{\perp} , the degrees of longitudinal and transverse polarizations of neutralino P_{II} and P_{\perp} in the $\tilde{\chi}_2^- \Rightarrow \tilde{\chi}_1^0 + H^-$ decay at $M_A = 180$ GeV, $2M_1 = M_2 = 150$ GeV, $\tan\beta = 1$, $M_Z = 91.1875$ GeV, $M_W = 80.385$ GeV, $\sin^2\theta_W = 0.2315$.

In fig. 8, a graph is presented that characterizes the dependence: longitudinal spin asymmetry A_{II} (at $\cos\theta = 1$); the degree of longitudinal polarization of neutralino P_{II} ; transverse spin asymmetry A_{\perp} (at $\sin\theta = 0.5$) on the chargino mass in the decay $\tilde{\chi}_2^- \Rightarrow \tilde{\chi}_1^0 + H^-$. As can be seen, with an increase in the chargino mass, the longitudinal spin asymmetry A_{II} , the degree of longitudinal polarization of neutralino P_{II} and A_{\perp} transverse spin asymmetry decrease.

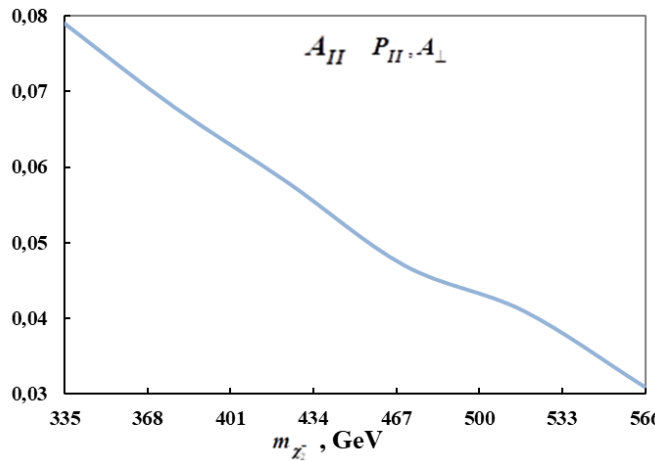


Fig. 8. Dependence of A_{II} (at $\cos\theta = 1$), P_{II} (at any θ) and A_{\perp} (at $\sin\theta = 0.5$) on the chargino mass

As for the degree of transverse polarization of neutralinos P_{\perp} , we note that they are almost insensitive to the mass of the charginos and amounts to 50% at the above values of the parameters.

Fig. 9 shows the angular dependence of A_{II} , A_{\perp} , P_{\perp} . It follows from the figure that the longitudinal spin asymmetry at the beginning of the angular spectrum is positive, with an increase in the angle θ it decreases and vanishes at $\theta = 90^\circ$, then it changes sign and increases in absolute value. The maximum value of the longitudinal spin asymmetry is observed at an angle $\theta = 0^\circ$ and is $A_{II} = 7.9\%$. The transverse spin asymmetry A_{\perp} is positive; it increases with increasing angle θ , reaches a maximum at the angle $\theta = 90^\circ$ and is $A_{\perp} = 10\%$; a further increase in the angle θ leads to a decrease in the asymmetry A_{\perp} . The degree of transverse polarization of neutralino is negative, with increasing angle θ decreases and reaches -1 at angle $\theta = 90^\circ$, and then increases in magnitude with increasing angle.

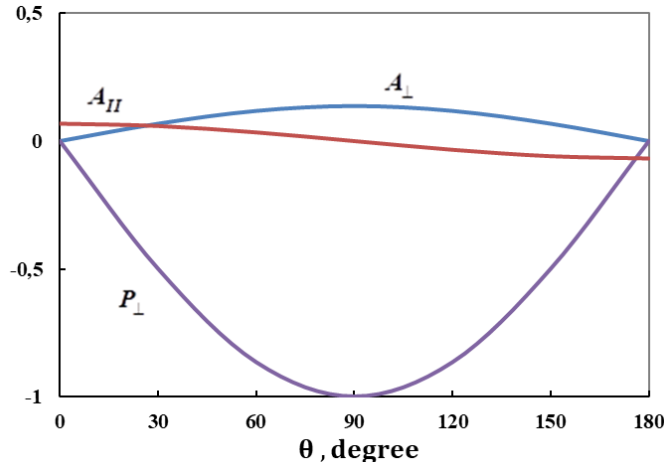


Fig. 9. Dependence of A_{II} , A_\perp and P_\perp on the angle θ at a chargino mass $m_{\tilde{\chi}_2^{\pm}} = 378.303$ GeV

4. Conclusion

We have discussed the decays of a heavy chargino (neutralino) to a light chargino (neutralino) and a Higgs boson: $\tilde{\chi}_2^\mp \Rightarrow \tilde{\chi}_1^\mp + h(H; A)$, $\tilde{\chi}_{3,4}^0 \Rightarrow \tilde{\chi}_{1,2}^0 + h(H; A)$, $\tilde{\chi}_2^\pm \Rightarrow \tilde{\chi}_1^0 + H^\pm$. In the framework of the Minimal Supersymmetric Standard Model and taking into account the polarization states of the chargino (neutralino), analytical expressions for the decay width are obtained. The degrees of the longitudinal and transverse polarizations of the chargino (neutralino), as well as the asymmetry caused by the longitudinal and transverse polarization of the initial chargino (neutralino), were determined. The dependence of these characteristics and the decay width on the chargino (neutralino) mass has been studied in detail.

REFERENCES

1. ATLAS Collaboration. *Observation of a new particle in the search for the Standard Model Higgs boson with the ATLAS detector at the LHC*, Phys. Lett., 2012. B 716, p. 1-29.
2. CMS Collaboration. *Observation of a new boson at a mass of 125 GeV with the CMS experiment at the LHC*, Phys. Lett., 2012. B 716, p. 30-61.
3. Rubakov V. A. *On Large Hadron Collider discovery of a new particle with Higgs boson properties* // UFN, 2012, V. 182, № 10, p.1017-1025 (in Russian).
4. Boos E. E. *Standard Model and predictions for Higgs Boson* // UFN, 2014, V. 184, № 9, p. 986 – 996 (in Russian)
5. Lanev A. V. *CMS Collaboration results: Higgs boson and search for new physics* // UFN, 2014. V. 184, № 9, p.996 – 1004 (in Russian).
6. Kazakov D. I. *The Higgs boson is found: what is next?* // UFN, 2014, V. 184, № 9, p.1004 – 1016 (in Russian).
7. Higgs P. W. *Broken Symmetries and the masses of gauge bosons.* // Phys. Rev. Letters, 1964, V.13, № 16, p. 508.
8. Englert F., Brout R. *Broken Symmetry and the mass of gauge vector bosons.* // Phys. Rev. Letters, 1964, V.13, №9, p.321
9. Gunion J. F., Haber H. E. *CP – conserving two – Higgs – doublet model : The approach to the decoupling limit* // Phys. Rev., 2003, V. D. 67, p. 0750.19.
10. Branco G. C. // Phys. Rep., 2012, V.516, p.1.
11. Djouadi A. *The Anatomy of Electro-Weak Symmetry Breaking. Tome II: The Higgs boson in the Minimal Supersymmetric Standard Model.* arXiv: hep-ph/ 0503173v2, 2003.
12. Gunion J. F., Haber H. E., *Higgs bosons in supersymmetric models (I)* // Nuclear Phys. 1986, B272, p.1-76.
13. Kazakov D. I. *Supersymmetry on the run : LHC and dark matter* // Nucl. Phys. B Procc. Suppl. 2010, V. 203 – 204, p.118.

14. Djouadi A., Kalinowski J., Zerwas P. M. // Phys. Lett. , 1996, V. B. 376., p. 220.
15. Djouadi A., Kalinowski J., Ohmann P., Zerwas P. M // Heavy SUSY Higgs bosons at $e^- e^+$ linear colliders // Z. Phys., 1997, V. C. 74, p. 93 -111.
16. Djouadi A., Janot P., Kalinowski J., Ohmann P., Zerwas P. M. SUSY Decays of Higgs Particles. Preprint, 1996, CERN PPE / 96 – 34, 13 p.
17. El Kheishen M. M., Shafik A. A., Aboshousha A. A. Analytic formulas for the neutralino masses and the neutralino mixing matrix. // Phys. ReV., 1992 , V. D. 45, №11, p. 4345 - 4348.
18. Spira M. QCD effects in Higgs physics . arXiv : hep – ph / 9705337v2, 1997, CERN – TH / 97 – 68, 101 p.
19. Djouadi A., Kalinowski J., Zerwas P. M. Two – and Three – Body Decay Modes of SUSY Higgs Particles arXiv : hep – ph / 9511342v1, 1995.
20. Abdullayev S. K., Omarova E. Sh. Two and three particle decay channels of supersymmetric Higgs bosons., Azerb. Journal of Physics Fizika, 2019. Vol. XXV , №4, p. 29 -39.
21. Abdullayev S. K., Omarova E. Sh. Decays of Higgs boson into a gauge boson and a fermion – antifermoin pair // Russian Physics Journal , 2019, V. 62, №1, p.30-38.
22. Abdullayev S. K., Omarova E.Sh. Three – particle decays of the Higgs Bosons in the Minimal Supersymmetric Standard Model // Russian Physics Journal, 2019, V.62, №3, p. 425 – 435.
23. Abdullayev S. K., Omarova E.Sh. Decay Channels of Higgs Bosons $H(h;A) \Rightarrow \gamma\gamma$, $H(h;A) \Rightarrow \gamma Z$, $H^\pm \Rightarrow \gamma W^\pm$ // Journal of Baku Engineering University – Physics, 2019, V.3, №1, p. 39 – 57.
24. Abdullayev S. K., Omarova E.Sh. Decay of the heavier chargino into lighter chargino and Higgs boson // Russian Physics Journal , 2020 (in press).
25. Abdullayev S. K., Omarova E.Sh. The decay of chargino into neutralino and Higgs – boson // Russian Physics Journal , 2020 (in press).
26. Haber H., Kane G. The Search For Supersymmetry : Probing Physics Beyond The Standard Model // Phys. Rept. 1985, V.117, p.75.

PACS:61.05.-a

Uot: 539.196.3

SPATIAL AND ELECTRONIC STRUCTURES OF HYLAMBATIN (8-12) PENTAPEPTIDE

G.A. AGAEVA¹, G.R.SAFARLI², N.M.GODJAEV^{2,3}

1-Institute for Physical Problems, Baku State University ,

AZ-1148, Baku, Z.Khalilov Str.23, Azerbaijan

2-Baku State University , AZ-1148, Baku, Z.Khalilov Str.23, Azerbaijan

3-Baku Engineering University, AZ-0101,Baku -Sumqait Road,16 km, Azerbaijan

*gulshen@mail.ru***ABSTRACT**

The spatial and electronic structure of C-terminal pentapeptide of hylambatin molecule have been investigated by computer modeling methods. It is shown that this molecule has preferred alpha-helical conformational state. This peptide preferentially adopt the quasicyclic conformation, stabilized by hydrogen bonds between the end groups of molecule. The energy and geometrical parameters and for each of low-energy conformations are obtained. The important stable inter-residue interactions of preferred conformations of this molecule were calculated. By means of semiempirical quantum-chemical method have been determined the electronic characteristics and values of dipole moments of all low-energy conformations of C-terminal pentapeptide.

Keywords: hylambatin , pentapeptide, spatial structure, electronic structure, conformation.

ПРОСТРАНСТВЕННАЯ И ЭЛЕКТРОННАЯ СТРУКТУРЫ МОЛЕКУЛЫ ГИЛАМБАТИНА (8-12)**РЕЗЮМЕ**

Пространственная и электронная структуры молекулы С-концевого пентапептида гиламбатина исследована компьютерными методами моделирования. Показано, что эта молекула предпочтительно укладывается в альфа-спиральное конформационное состояние. Энергетически предпочтительная конформация молекулы образует квазициклическую структуру, стабилизированную водородными связями между конечными группами основной цепи молекулы. Для каждой из низкоэнергетических конформаций пентапептида получены энергетические и геометрические параметры. Были вычислены величины энергетических вкладов межстаточных взаимодействий в оптимальных конформациях молекулы. Посредством полуэмпирического квантово-химического метода, определены электронные характеристики и величины дипольных моментов всех низкоэнергетических конформаций молекулы С-концевого пентапептида гиламбатина слова.

Ключевые: гиламбатин, пентапептид, пространственная структура, электронная структура, конформация.

HİLAMBATİN (8-12) MOLEKULUNUN FÖZA VƏ ELEKTRON GURULUŞLARI**XÜLASƏ**

Hilambatin (8-12) pentapeptid molekulunun fəza və elektron quruluşları molekulyar modelləşdirmə üsulları ilə tədqiq edilmişdir. Göstərilmişdir ki, bu molekul enerji cəhətdən alfa-spiral konformasiya vəziyyətinə meyli edir. Bu pentapeptid molekulun ən stabil konformasiyası hidrogen rabitələri ilə sabitləşmiş, kvazitsiklik quruluş əmələ gətirir. Molekulun hər bir aşağı-enerjili konformasiyası üçün enerji və həndəsi parametrlər hesablanmışdır. Bütün optimal konformasiyalarda qalıqlar arası qarşılıqlı təsirlərin enerji payları hesablanmışdır. Yarımempirik kvant kimyəvi hesablama üsulu vasitəsi ilə bu pentapeptid molekulunun aşağı-enerjili quruluşlarının elektron xarakteristikaları və dipol momentləri müəyyən edilmişdir.

Açar sözlər: hilambatin, pentapeptid, fəza quruluşu, elektron quruluşu, konformasiya.

I. INTRODUCTION

The knowledge of preferred conformations and electronic structure of pharmacologically active peptides is necessary information for understanding of their mechanism of action. Hylambatin (Hyl), a dodecapeptide isolated from the skin of the African frog, *Hylambates maculatus*, belongs to the family of tachykinin or physalaemin-like peptides. Hylambatin (DPPDPNRFYGMamide) is the first example of a tachykinin which possesses a methionyl methionine residue at the C-terminus, rather than the C-terminal tripeptide -Gly-Leu-Met-NH₂ which hitherto has been a characteristic feature of all members of the tachykinin family [1-3]. It is well known that the C-terminal pentapeptide amide in the tachykinin family represents the minimum requirement for the appearance of full tachykinin-like bioactivity (1), and it is a well established fact that all tachykinins hitherto found in nature (in molluscan tissues, amphibian skin and mammalian tissues) contained the common C-terminal tripeptide -Gly-Leu-Met-NH₂. Hylambatin, with its C-terminal tripeptide, -Gly-Met-Met-NH₂; represents a unique exception to this rule. The pharmacological study of hylambatin is in progress and the preliminary results indicated that the spectrum of activity of hylambatin seems similar to that of physalaemin rather than to that of kassinin the other tachykinin peptide. Except this the effect of hylambatin on the secretion of glucoregulatory hormones was examined in the rat. Hylambatin, injected intravenously in graded doses 10 and 30 min before blood collection, significantly increased both plasma glucose and plasma insulin, whereas the secretion of glucagon was not affected. This profile of action is different from that of kassinin or substance P. Should hylambatin, like other neuropeptides, be present in mammalian tissue, it may have a role in the regulation of carbohydrate metabolism activity [4,5].

The major aim of the present article is the investigation of the preferred conformations and electron structure for C-terminal pentapeptide for hylambatin, with the purpose of getting insight into basic structural requirement that determine ligand-receptor interaction. The conformational analysis of this pentapeptide have been carried out by molecular mechanic method, which allow to determine a whole sets of energetically preferred conformers of peptide molecule, but the charge distribution and dipole moments of peptide conformations was obtained by means of semiempirical quantum-chemical method.

II. STRATEGY AND METHOD

Molecular mechanics method

The conformational energy is considered the sum of independent contributions of nonbonded E_{nb}, electrostatics E_{el}, torsional interactions E_{tor} and hydrogen bonding E_{hb} energies. The first term is described by the Lennard-Jones potential with the parameters proposed by Scheraga [6]. The electrostatic energy is calculated in a monopole approximation, with atom centered charges obtained by Momany et al [7,8]. The dielectric constant is assumed to equal ten [9]. Torsional potentials and barriers to rotation about bonds N-C^α (φ), C^α-C' (ψ), C'-N (ω), and about side chain bonds C^α-C^β (χ) were as proposed by Scheraga [6]. The hydrogen bond energy calculated from the Morse potential [10] are supposed to be weakened with maximum energy of 1.5 kcal/mol. Bonding lengths and angles are those given Corey and Pouling. Above potentials with energy and geometry parameters are used in some investigations. Conformational energy was calculated with a computer using program writteen by Godjayev et al [10,11]. The conventions used for torsion angles are those of IUPAC-IUB Commission [12].

CNDO/2 method

The shape of a molecule is often associated with a surface of constant charge density. An atomic partial charge distribution is an essential element of any force field for peptide ligands. The peptides electronic structure was investigated, the active site, the way of action and structure-activity relationship were discussed. These molecules not only may have the same way of action but also may have common site of action in the receptor when they interact with this receptor. The ensemble of charges, or an equivalent collection of multipoles, not only describes the external molecular field, but its self-energy - taking induction into account - also represents an important component of the internal molecular energy. We uses CNDO/2 for the determination of electronic charge density for the molecules. Complete Neglect of Differential Overlap (CNDO) is the simplest of the SCF methods for semi-empirical quantum mechanics calculations. It is useful for calculating ground-state electronic properties of open- and closed-shell systems, geometry optimization and total energy [13,14]. Method CNDO/2 gives a correct charge distribution in peptide molecules and more or less satisfactory describes such their features, as dipole moments and total energy of molecules. We calculates charge density as a sum of molecular orbital densities, each the square of the orbital wave function. In this study we investigate how the charge distribution of a molecule may be related with their reactionary ability. An atomic partial charge distribution of the stable conformation of molecules allow to predict the relationships of their reactionary ability with separate molecule areas. Here we will only be considering the charge distribution itself, leaving aside for the moment a discussion of intramolecular electrostatic and polarization energies and their relation to intermolecular interaction energies.

III. RESULTS AND DISCUSSION

Conformational study of the C-terminal pentapeptides of the hylambatin (Phe-Tyr-Gly-Met-Met) molecule was carried out, basing on the fragmental analysis. The initial variants of the small fragments were formed on the base of low-energy conformations of the corresponding monopeptides. Conformational analysis of pentapeptides Phe-Tyr-Gly-Met-Met has been carried out basing on the 10 most stable conformations of the preceding dipeptides Phe-Tyr and Met-Met and 4 low-energy conformations of Gly monopeptide. For this pentapeptide were analyzed 400 conformations belonging to 16 different shapes. Each of these low-energy conformations comprises a lowest structures of the preceding dipeptides. Molecular mechanics study of C-terminal pentapeptides has shown that its spatial structure may be described by similar families of low-energy conformations. The calculated conformations of the other possible shapes are energetically much less favourable, their energy being 3 kcal/mol higher than the global structure. For this pentapeptide global conformation adopt a helical structure. Only helical structures of the pentapeptides are fall in the 0-3 kcal/mol relative energy interval. It is shown that all preferred pentapeptide conformations have similar backbone form and orientations of side chains at the C-terminal part of molecule. The calculated values of dihedral angles of rotation about the backbone and side chains bonds in the global conformation of the pentapeptide and its relative energy values and important hydrogen bonds are given in Table1.

Table1. The energy parameters of low-energy conformations of C-terminal pentapeptide of hylambatin molecule.

Residue	Conformation
Dihedral angles	$\phi, \psi, \omega, \chi_1, \chi_2, \chi_3, \chi_4$.
Phe	-64,-45, 178, 180,91
Tyr	-74,-32, 176, 180, 90, 180
Gly	-63, -39, 182
Met	-82, -55, 182, 181, 173,180, 180
Met	-87, -53, 179, -60, 183,180, 181
E_{rel} (kcal/mol)	0
Important hydrogen bond (length, energy)	(Met ⁵) NH...OC(Phe ¹) (1.7 Å, 1.1 kcal/mol)

The lowest energy structure of pentapeptide formed by most favourable nonvalent interactions and therefore may become the most preferred in a strongly polar medium. Calculation showed that in global helical conformation of pentapeptide is formed a identical hydrogen bond between atoms of the backbone of the Met⁵ and Phe¹ (Table 1) as in global conformations of homological C-terminal pentapeptide of tachykinin peptides. These hydrogen bonds play a significant role in stabilization of the helical spatial structure of this pentapeptide. Our calculations demonstrated that this C-terminal pentapeptide under the native conditions is not a fluctuating formation, but a compact structure with severely restricted conformational freedom. The most stable conformations of pentapeptide generally exhibit the similar backbone form and adopt the stable pentapeptide quasicyclic structure. The above calculation shows interesting conformational features of this pentapeptide which might be important for its biological activity. The preferred spatial structures of the C-terminal pentapeptide of the hylambatin are presented in Figure1 (a).

Quantum chemical calculations of the peptides.

The electronic parameters of the global conformations of the C-terminal pentapeptide (Phe-Tyr-Gly-Met-Met) of hylambatin molecule have been investigated using semiempirical quantum chemical calculations method. Optimal lowest energy conformations of these peptide were determined by molecular mechanics method, but the atomic charges and dipole moments were calculated by molecular orbital calculations method CNDO/2 with standard parametrization. The charge distributions in the global conformation of this pentapeptide are represented in the Fig 1 (b). Both Phe and Tyr residues have the aromatic side chain , but yet in side chain of Tyr exist a hydroxyl group OH and this factor possible is an essential for peptide interaction with selective receptor. The results of quantum chemical calculation show that in lowest energy conformation of the peptide the total dipole moment totally differs one from another low-energy conformations. Table 2 summarized the result of the total electron energy calculations of the investigated pentapeptide molecule. The calculation results are coinciding with conformational analysis data. Therefore in global conformation the side chain of the Phe¹ residue is in fixed state. Hydrogen bonding is to increase the values of the partial positive and negative charges somewhat and thus accentuate the electrostatic components of the interaction between the side chains of the Phe¹ and Met⁵ residues. In other words, these interactions are more electrostatic.

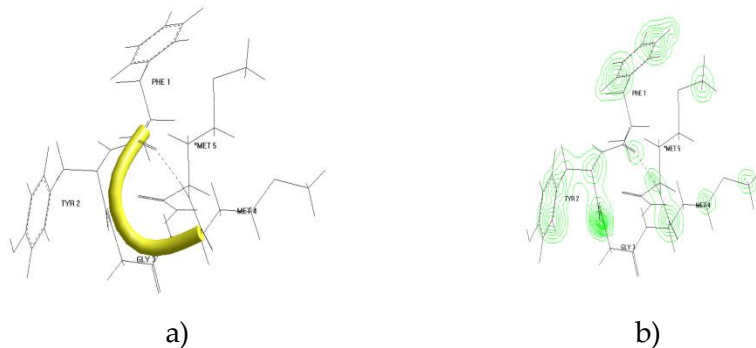


Fig.1. Preferred spatial structures of the C-terminal pentapeptides of the hylambatin molecule (hydrogen bond is shown dashed line, peptide backbone is shown yellow line).

TABLE 2. The energy parameters and summary dipole moments of electronic structure of the lowest energy conformation of hylambatin C-terminal pentapeptide.

Electronic parameters of electronic structure of the preferred α -helical conformation	
Total energy, kcal/mol	-183631
Binding energy, kcal/mol	-8159
Isolated atomic energy, kcal/mol	-175472
Electronic energy, kcal/mol	-2055843
Core-Core interaction energy, kcal/mol	1872212
Heat of formation, kcal/mol	376
Dipole moment, debyes (D)	8

Results representing the distribution of electrostatic energy derived from quantum chemical calculations show that different parts atom groups have different amounts of charge density, so it could be said to be difficult to represent the Tyr hydroxyl group as having some negative charge. However, the results show that the most positive part is at the surface immediately opposite to the hydroxyl group, so the these dipoles is still evident with this approach (Table2). The electronic structure of both pentapeptides indicate a similar charge distribution around the C-terminal group and imply that their binding to the receptor site could be similar (Fig.1 (b).). On the basis of this investigation may also consider spatial structure other tachykinins with common C-terminal pentapeptide. They not only have the same way of action but also have common site of action in the receptor when they interact with receptor.

CONCLUSIONS

Comparison of results of the calculations showed that C-terminal pentapeptides of hylambatin molecule under polar conditions is not a fluctuating formation, but a compact structure with severely restricted conformational freedom. Calculation show in global helical conformation of this pentapeptide is formed a identical stable hydrogen bond between atoms of the backbone of the Met⁵ and Phe¹ as in some tachykinin C-terminal pentapeptides. These hydrogen bonds play a significant role in stabilization of the helical spatial structures of this pentapeptide. The most stable conformations of hylambatin C-terminal pentapeptide generally exhibit the similar backbone form and adopt the stable pentapeptide quasicyclic structure. The results of quantum chemical calculation showed that this molecule have similar preferred conformational states with different electronic structure. The above calculation shows interesting conformational features of this pentapeptide which might be important for its biological activity.

REFERENCES

1. Yasuhara T, Nakajima T, Falconieri Erspamer G, Erspamer V (1981). New tachykinins Glu2,Pro5-kassinin (Hylambates-kassinin) and hylambatin in the skin of the African rhacophorid frog *Hylambates maculatus*. *Biomed Res.*, vol.2, p.613–617
2. Güllner HG, Harris V, Yajima H, Unger RH (1984). Hylambatin, a structurally unique tachykinin: effects on insulin and glucagon secretion. *Arch. Int. Pharmacodyn. Ther.*, vol.272(2), p.304-309.
3. Inoue A, Fukuyasu T, Nakata Y, Yajima H, Nomizu M, Inagaki Y, Asano K, Segawa T (1988). Structure-activity relationship of hylambatin and its fragments as studied in the guinea-pig ileum. *J. Pharm. Pharmacol.*, vol. 40(1), p.72-73.
4. Falconieri Erspamer G, Mazzanti G, Yasuhara T, Nakajima T (1984). Parallel bioassay of physalaemin and hylambatin on smooth muscle preparations and blood pressure. *J. Pharm . Pharmacol.*, vol.36(4), p.284-286.
5. Inoue A., Fukuyasu T., Nakata Y., Yajima H., Nomizu M., Inagaki Y., Asano K., Segawa T. Structure-activity relationship of hylambatin and its fragments as studied in the guinea-pig ileum. *Journal of Pharmacy and Pharmacology*, 1988 ,vol.40, Iss.1, p.72-73
6. Scheraga H.A. Recent progress in the theoretical treatment of protein folding , *Biopolymers*, 1983, vol. 22, pp.1-14
7. Popov E.M. Quantitative approach to conformations of proteins , *Int. J. Quant. Chem.*, 1979, v.16, p. 707-737
8. Momany F.A., Mc.Guire R.F., Burgess A.W., Scheraga H.A. Energy parameters in polypeptides : VII. Geometric parameters, partial atomic charges, nonbonded interaction for naturally occurring amino acid , *Phys. Chem.*, 1975, vol. 79, p. 2361-2381
9. Агаева Г.А., Агаева У.Т., Годжаев Н.М., Особенности пространственной организации молекул гемокинина-1 человека и гемокинина-1 мыши/крысы. Биофизика (Russian), Москва, 2015, том 60, вып. 3, с. 457–470
10. Максумов И.С., Исмаилова Л.И., Годжаев Н.М. Программа полуэмпирического расчета конформаций молекулярных комплексов на ЭВМ , *Журнал структурной химии*, т.24, №4, 1983, с. 147-148
11. Годжаев Н.М., Максумов И.С. Алгоритм расчета конформаций биополимеров , Уч. записки АГУ, серия физ-мат. наук, 1979, №5, с.157-162
12. IUPAC-IUB Commision on Biochemical Nomenclature Abbreviations and symbols for description of conformation of polypeptide chains , *Pure Appl. Chem.*, 1974, vol. 40, p. 291-308
13. Pople J.A., Segal G.A., Approximate self-consistent molecular orbital theory. II. Calculations with complete neglect of differential overlap, *J.Chem.Phys.*, 1965, vol.43, p.136–149
14. Pople J.A., Segal G.A., Approximate Self-Consistent Molecular Orbital Theory. III. CNDO Results for AB₂and AB₃ Systems, *J.Chem.Phys.*, 1966, vol.43, p.3289–3296

IOT 621.315.592PACS:65.40.-b

ELECTRONIC SPECTRUM OF α -In₂Se₃ COMPOUND AND NATURE OF THE CHEMICAL BONDS

E.M. QOCAYEV¹, Z.A. CAHANGIRLI^{2,3}, A.F.GARIBLI⁴, S.A. NABIYEVA^{2,5}

¹Azerbaijan Technical University

² Institute of Physics of Azerbaijan National Academy of Sciences

³Baku State University

⁴Sumgayit State University

⁵Academy of the Ministry of Emergency Situations of the Azerbaijan Republic

talibli_aysel@mail.ru

ABSTRACT

In the article a band structure and energy density of the α -In₂Se₃ crystal using Density Functional Theory (DFT) have been calculated and on their base a genesis of chemical bonds in this crystal has been determined. Based on the electronic band structure it was determined that α - In₂Se₃ is a semiconductor compound with a band gap of 0.9 eV. The valence band is divided into three groups. From the analysis of the wave functions of the valence bands it is obtained that the bands around -15 ÷ -11 eV are derived from the s-states of the Se atom. The bands near -5 eV are mainly formed from the s-states of the In atom and p-states of the Se atom. Finally, the highest group around - 4 ÷ 0 eV forms from the p-states of the Se atom with a small mixture of the p-states of the In atom.

Keywords: α -In₂Se₃, DFT, band structure, energy density, chemical communication, electronic spectrum

ЭЛЕКТРОННЫЙ СПЕКТР СОЕДИНЕНИЯ α -In₂Se₃ И ПРИРОДА ХИМИЧЕСКИХ СВЯЗЕЙ

РЕЗЮМЕ

В статье рассчитаны зонная структура и плотность энергии кристалла α -In₂Se₃ с использованием теории функций плотности (DFT) и на их основе определен генезис химических связей в этом кристалле. На основании электронной зонной структуры было определено, что α -In₂Se₃ представляет собой полупроводниковое соединение с шириной запрещенной зоны 0,9 эВ. Валентная полоса делится на три группы. Из анализа волновых функций валентных зон получается, что зоны около -15 ÷ -11 эВ являются производными s-состояний атома Se. Полосы около -5 эВ в основном образованы s-состояниями атома In и p-состояниями атома Se. Наконец, высшая группа около -4 ÷ 0 эВ образуется из p-состояний атома Se с небольшой смесью p-состояний атома In.

Ключевые слова: α -In₂Se₃, DFT, зонная структура, плотность энергии, химическая связь, электронный спектр

α -In₂Se₃ BİRLƏŞMƏSİNİN ELEKTRON SPEKTRI VƏ KİMYƏVİ RABİTƏNİN TƏBİƏTİ

XÜLASƏ

Məqalədə Sixlıq Funksionalı Nəzəriyyəsindən (DFT) istifadə etməklə α -In₂Se₃ kristalının zona quruluşu, energetik hal sixlığı hesablanmış və onların əsasında bu kristalda kimyəvi əlaqələrin genezisi təyin olunmuşdur. Elektron zona quruluşu əsasında müəyyən edilmişdir ki, α - In₂Se₃ qadağan zolağı 0.9 eV olan yarımkəciri birləşmədir. Valent zonası üç qrupa bölünür. Valent zonalarının dalğa funksiyalarının analizindən alınır ki, -15 ÷ -11 eV ətrafında yerləşən zonalar Se atomunun s-hallarından törəmişdir. -5 eV yaxınlığında zonalar əsasən In atomunun s-, Se atomunun isə p-hallarından formalaşır. Nəhayət, -4 ÷ 0 eV ətrafındakı ən yuxarı qrup In atomunun p-hallarının azacıq qarışıqlığı olmaqla, Se atomunun p-hallarından əmələ gəlir.

Açar sözlər: α - In₂Se₃, DFT, zona quruluşu, energetik hal sixlığı, kimyəvi rabitə, elektron spektri

Introduction

Chalcogenides form a large group of two-dimensional layered materials with different electronic and optical properties. These include metals, semiconductors and topological insulators. As is typical for 2D layered materials, their electronic and optical properties are highly dependent on the number, sequence, and location of atoms within the layer [1]. The In_2Se_3 compound is a widely used member of this type of substance. This compound has many technological applications, including solar cells [2], photodetectors [3] and phase transition memory devices.

Although the In_2Se_3 crystal has been studied for many years, information about its crystal structure is often quite confusing and even contradictory [4]. Thus, there are differences of opinion regarding the atomic coordinates within the layer and the sequence of layers position. At least four phases of this compound (α , β , γ and δ) are known. One of them - phase δ has a 3D, and the others have a 2D layered structure. Layered structures are composed of Se-In-Se-In-Se atomic layers. Within each of the five layers, a strong covalent bond between the atoms, and van der Waals interaction between the layers exist (Figure 1).

The value of the band gap obtained from the optical absorption spectra of the layered In_2Se_3 crystal and from ab-initio calculations based on the Functional Density Theory varies from 0.55 eV to 1.5 eV, and there are also conflicting reports on whether this substance is semiconductor with direct or indirect transitions. It is known that the DFT method reduces the band gap. Therefore, the mBJ (modified Becke-Johnson) potential [5] and the GGA (generalized gradient approximation) [6] were used in the calculations to accurately estimate the band gap.

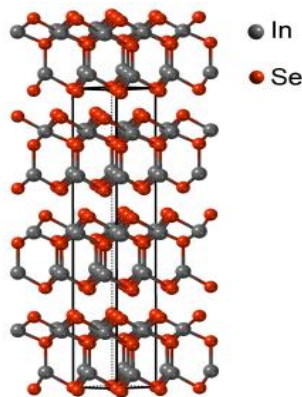


Figure 1. Crystal structure of α - In_2Se_3 compound.

Electronic spectrum and chemical bonds

The band structure and energy density of the α - In_2Se_3 crystal were calculated using the Wien2k [7] software package using the ab-initio DFT and FP LAPW (Full Potential Augmented Plane Wave) method. In the calculations, the "muffin-tin" radii of the In and Se atoms were taken equal to 2.5 Bohr. Within the muffin-tin sphere, the charge density and potential are expanded into spherical harmonics with $L_{\max} = 10$. In the space between the spheres, the wave functions are expanded into Fourier series and $R_{\text{MT}}K_{\max} = 8$ is taken to obtain the required energy convergence, here R_{MT} is the average radius of the "muffin-tin" sphere, K_{\max} is the maximum value of the inverse lattice vector. The calculations used 350 points from the irreducible part of the Brillouin zone. Convergence accuracy of total energy and specific values was 10^{-5} eV.

Band structure calculations were performed at symmetrical points G, Z, F ~ and L and along the lines connecting them (Figure 2). As can be seen from Figure 2, the width of the valence band is approximately -15 eV and it can be divided into three main groups. The maximum of the valence band (VBM) is located along the line Γ – L at a distance of about one third of the segment Γ - L from the point Γ . The minimum of the conduction band (CBM) is located at point Γ . Thus, it is derived from our calculations that the α -In₂Se₃ crystal is a semiconductor with indirect transition with a bandwidth of ~0.9 eV. The direct transition situated at point Γ is equal to ~1 eV.

In order to study the genesis of electronic energy states - the nature of chemical bonding, energy state densities projected on individual atoms were calculated (Figure 3.). From the analysis of the energy state densities and the expansion of the wave functions of the bands, it is obtained that the lowest valence bands around -15 ÷ -10 eV are derived from the s-states of Se atom. Because these bands are energetically very deep relative to the maximum of the valence band, they do not participate in optical transitions and do not form the semiconductor properties of the α -In₂Se₃ crystal. The next group of bands below the maximum of the valence band -5 eV is formed mainly by the s-states of In atom and p-states of Se atom.

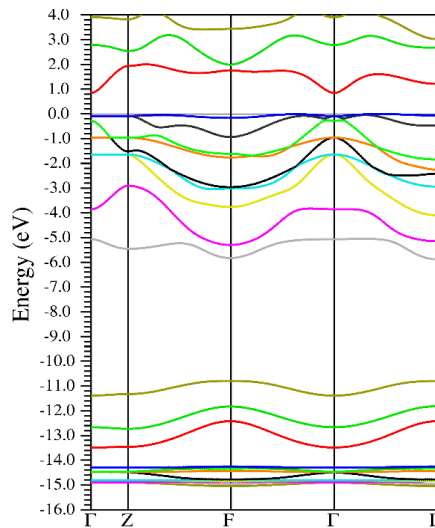


Figure 2. Band structure of the α -In₂Se₃ crystal.

Finally, the highest group in the energy range -4÷ 0 eV is formed from the p-states of the Se atoms, with a small mixture of the p-states of In atoms. As can be seen from Figure 3, the minimum of the conduction band is mainly formed from the s-states of In atom and the p-states of Se atom.

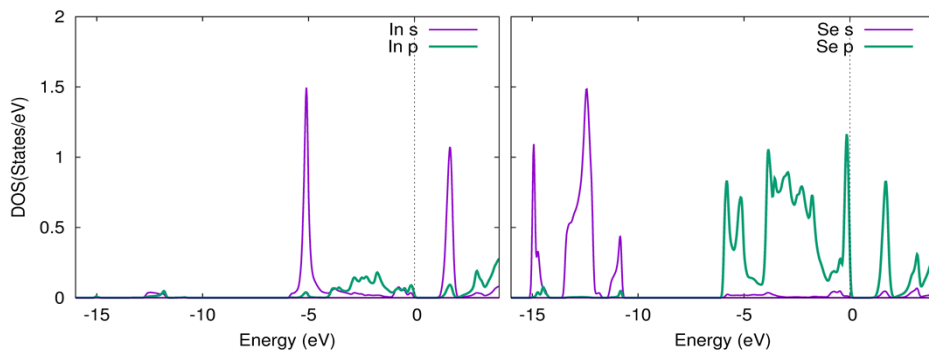


Figure 3. Energy state densities of α -In₂Se₃ crystal projected on atoms.

Conclusion

Ab-initio calculations have shown that α -In₂Se₃ crystal is a semiconductor with indirect transition with a bandwidth of ~0.9 eV. The maximum of the valence band is located on the line Γ - L. The direct transition at point Γ is equal to ~1 eV. The minimum of the conduction band is located at point Γ . The analysis of the energy state densities projected on the atoms shows that the maximum of the valence band is formed from the p-states of the Se atom, with a small mixture of the p-states of In atom. The minimum of the conduction band is formed mainly by the s-states of In atom and p-states of the Se atom.

REFERENCES

1. J. E. Padilha, H. Peelaers, A. Janotti, and C. G. Van De Walle, Nature and evolution of the band-edge states in MoS₂: From monolayer to bulk, *Physical Review B* 90, 205420 (2014).
<https://doi.org/10.1103/PhysRevB.90.205420>
2. H. Peng, D. T. Schoen, S. Meister, X. F. Zhang, and Y. Cui, Synthesis and Phase Transformation of In₂Se₃ and CuInSe₂ Nanowires, *Journal of the American Chemical Society* 129, 1, 34-35 (2007).
<https://doi.org/10.1021/ja067436k>
3. N. Balakrishnan, C.R. Staddon, E.F. Smith, J. Stec, D. Gay, G.W. Mudd, O. Makarovsky, Z.R. Kudrynskyi, Z.D. Kovalyuk, L. Eaves, and A. Patane, Quantum confinement and photoresponsivity of β -In₂Se₃ nanosheets grown by physical vapour transport, *2D Materials*, vol.3, 1, 025030 (2016). <https://doi.org/10.1088/2053-1583/3/2/025030>
4. K. Osamura, Y. Murakami, and Y. Tomiie, Crystal Structures of α -and β -Indium Selenide, In₂Se₃, *Journal of the Physical Society of Japan*, 21, 1848 (1966). <https://doi.org/10.1143/JPSJ.21.1848>
5. F. Tran, P. Blaha. Accurate band gaps of semiconductors and insulators with a semilocal exchange-correlation potential. *Phys. Rev. Lett.* 2009, 102 (22), 226401. <https://doi.org/10.1103/PhysRevLett.102.226401>
6. J. P. Perdew, S. Burke, M. Ernzerhof. Generalized Gradient Approximation Made Simple *Phys. Rev. Lett.* 1996, 77, 3865. <https://doi.org/10.1103/PhysRevLett.77.3865>
7. Blaha, P., Schwarz, K., Madsen, G. K. H., Kvasnicka, D., Luitz, J., Laskowsk, R., Tran, F., Marks, L., & Marks, L. (2019). WIEN2k: An Augmented Plane Wave Plus Local Orbitals Program for Calculating Crystal Properties. Techn. Universitat. 287p. ISBN 3-950103112

PACS:77.22.Ej, 64.75 Bc, 31.70.Dk, 61.70 Og

ИОТ 532

ВЛИЯНИЕ НЕОРГАНИЧЕСКИХ СОЛЕЙ НА ФАЗОВУЮ ДИАГРАММУ И РАЗДЕЛИТЕЛЬНУЮ СПОСОБНОСТЬ ВОДНОЙ ДВУХФАЗНОЙ СИСТЕМЫ ПЭГ-НАТРИЕВАЯ СОЛЬ ЛИМОННОЙ КИСЛОТЫ-ВОДА

Э.А МАСИМОВ, Г.М ШАХБАЗОВА

Бакинский Государственный Университет

Азербайджан, г. Баку

В представленной работе были исследованы фазовые диаграммы водно-полимерной двухфазной системы ПЭГ-натриевая соль лимонной кислоты-вода и влияние некоторых неорганических солей на положения бинодалии и на величину разделительной способности двухфазной системы.

Ключевые слова: ПЭГ, натриевая соль лимонной кислоты, двузфазный систем.

THE INFLUENCE OF INORGANIC SALTS ON THE PHASE DIAGRAM AND SEPARATING ABILITY OF AQUEOUS TWO-PHASE SYSTEMS PEG-SODIUM CITRIC ACID-WATER

In the presented work, the phase diagrams of the water-polymer two-phase system PEG-sodium salt of citric acid-water and the concentration effect of the inorganic salt on the position of the binodal, on the value of the separating ability of the system were investigated.

Key words: PEG, sodium citric acid, two-phase systems.

Как известно [1], при смешивании растворов двух полимеров в общем растворителе (в частности в воде) при определенных условиях (в определенном интервале концентрации компонентов) происходит фазовое расслоение системы на две фазе различающиеся физико-химическими свойствами, в частности относительными гидрофобностями, в случае когда растворителем является вода. Следует отметить, что такая несовместимость компонентов в общем растворителе может наблюдаться и в смесях одного полимера с некоторыми неорганическими и органическими солями [2].

Систематические исследования А. Албертсона различных водно-полимерных двузфазных систем (ВПДС) [3] привели к появлению нового универсального, высокоеффективного, мягкого, экономически выгодного метода разделения (сепарации) и очистки самых различных биологических материалов.

Благодаря тому, что растворителем в обеих фазах системы является вода (70-80%), в такую систему можно вводить белки, нуклеиновые кислоты, вирусы, клетки и.т.д. Эти биологические объекты, в зависимости от их индивидуальных особенностей и от условий распределения (природы и концентрации фазообразующих компонентов, природы и концентрации добавок и.т.д.) неравномерно распределяются по существующим фазам, не теряя при этом своих интактных свойств.

Следует особо подчеркнуть, что этот метод успешно применяется также для количественной оценки относительной гидрофобности высокомолекулярных соединений которую невозможно было определить ранее существующими методами [6].

Для описания водных двухфазных систем принято изучать фазовую диаграмму системы (бинодальные кривые, соединительные линии, разделительскую способность и.т.д.). Свойства водной среды фаз двухфазной системы и характер фазовых диаграмм зависит от многих факторов: от природы и концентрации фазообразующих полимеров, их молекулярно-массовых характеристик, от природы и растворителя, температуры, присутствии низкомолекулярных добавок и.т.д.

Изучение влияния различных добавок, в частности неорганических солей на характеристики водно-полимерной двухфазной системы важно как с точки зрения, теории растворов, так и представляет очевидный практический интерес, так как добавки неорганических солей широко используется для регулирования процессов распределения биологических материалов в этих системах. Такого рода исследования проводились в работах [4,5] для двухфазных систем Д-ПЭГ, Д-ПВП, Д-Фиколл, Д- ПВС. В этих работах было показано, что степень влияния добавок неорганических солей на условия расслоения фаз в рассматриваемых двухфазных системах связано с положением соли в лиотропном ряду способности солей по осаждению белков в водных растворах. Однако, представляет интерес также изучение влияния неорганических солей на процесс расслоения в двухфазным системах полимер-органическая соль-вода.

В представленной работе были исследованы фазовые диаграммы водно-полимерной двухфазной системы ПЭГ-натриевая соль лимонной кислоты-вода и влияние неорганических солей на положения бинодалии и на величину разделительной способности системы.

На рис.1 представлена экспериментальные результаты описывающие бинодали и соединительные линии фазовой диаграммы изучаемой двухфазной системы в отсутствии и присутствии различных солей, где на рисунке по осям координант отложены весовые концентрации фазообразующих компонентов. Кривые диаграммы (бинодали) разграничают область существования гомогенных растворов (под бинодалью) и область существования гетерогенных (над бинодалью) растворов.

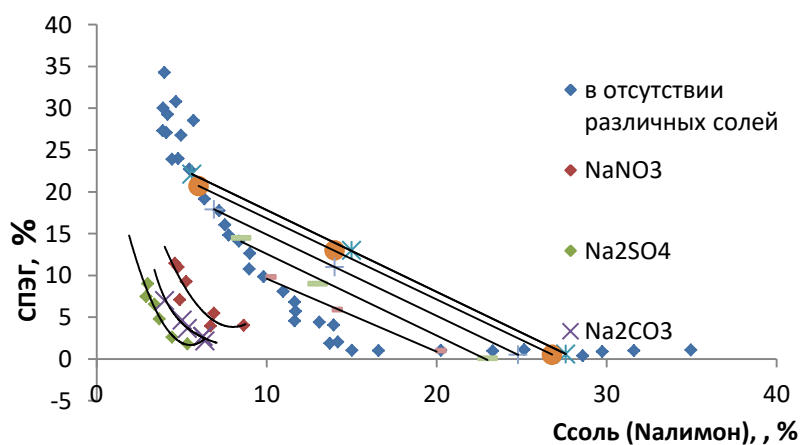


Рис. 1. Бинодалы фазовой диаграммы в отсутствии и присутствии добавленных солей

На рис.2. представлено изменения положения бинодали в присутствии соли (NaNO_3) различной концентрации.

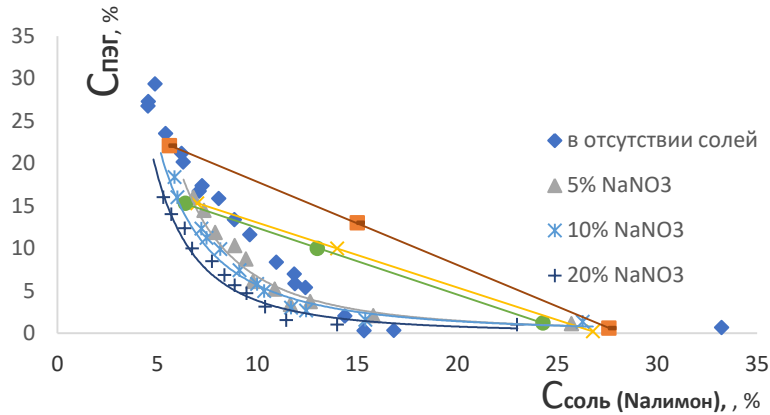


Рис2. Влияние соли (NaNO_3) на бинодали фазовой диаграммы водно двухфазной системы
ПЭГ-натриевая соль лимонной кислоты-вода

Как следует из полученных результатов добавлением всех солей в систему, бинодали фазовой диаграммы несколько смещаются в сторону начала координат, причем тем больше, чем больше концентрации соли (рис.2.). При этом увеличивается площадь гетерогенной области фазовой диаграммы. Таким образом разделение системы на две фазы наступает при меньших концентрациях фазообразующих компонентов, что свидетельствует о том что имеет место структурирования водной среды системы под влиянием добавленных солей. Очевидно, что структурование водной среды фаз двухфазной системы связано с изменением степени гидратации фазообразующих компонентов . При этом увеличивается различия свойств фаз, что в свою очередь приводит к худшей совместимости этих компонентов в общем растворителе, и естественно, к расслоению системы на две фазы при меньших концентрациях фазообразующих компонентов.

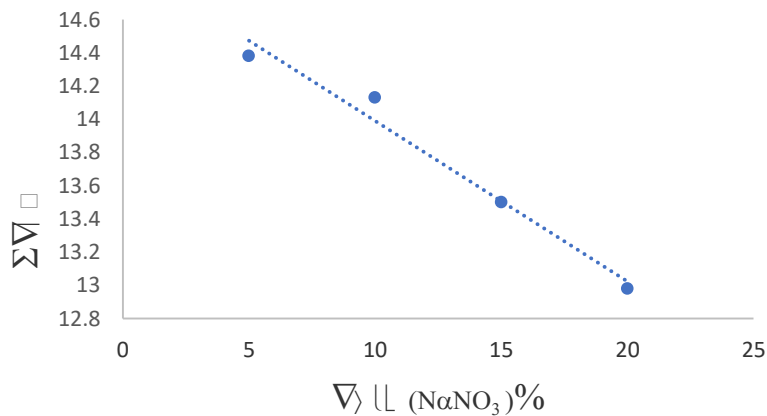


Рис3.

На рис.3 приведена зависимость суммарной концентрации фазообразующих компонентов в критической точке бинодал двухфазной системы под влиянием добавленной в систему соли (NaNO_3) различный концентрации. Полученные данные также свидетельствует о том, что под влиянием соли разделение системы на две фазы наступает при меньших суммарных концентрациях фазообразующих компонентов.

В работе было проведено сравнение между влиянием NaNO₃ на поверхностное натяжение воды и влияние идентичных концентрации этой же соли на суммарную концентрацию фазообразующих компонентов в критической точке бинодали двухфазной системы (где объемы фаз и концентрации компонентов в фазах равны). Результаты приведены на рис. 4 .

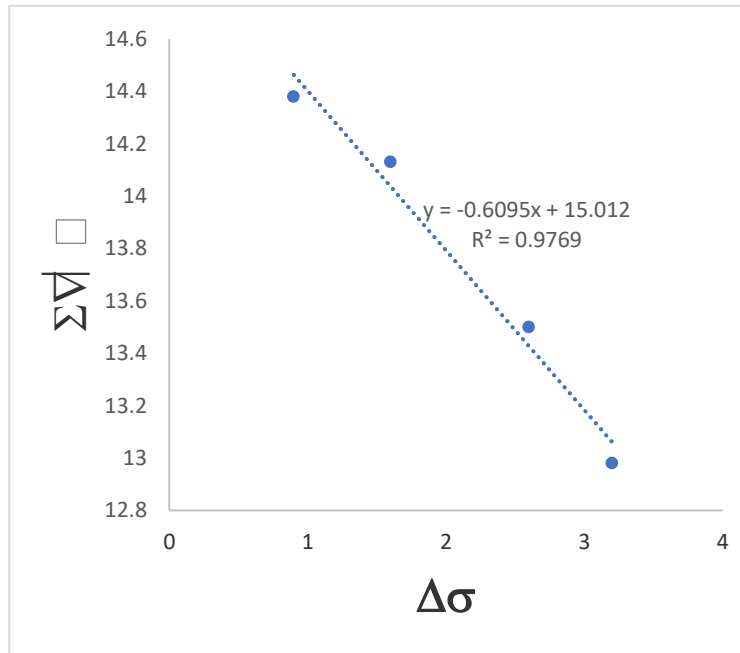


Рис.4.

Как следует из рисунка между этими параметрами существует определенная корреляционная связь. Этот результат также подтверждает о том, что добавленные соли в двухфазную систему структурирует водные среды двухфазной системы.

Для более подробного анализа полученных результатов рассмотрим механизм влияние солей на воду на основе теории Самойлова [9].

Согласно этой теории под ионом, (катионом или анионом) разрушающим структуру воды подразумевается ион, вблизи которого молекул воды обменивается с молекулами "свободной" воды в объеме с большей частотой, чем молекулы "свободной" воды между собой, т.е.

$$\nu_{(H_2O^0-H_2O^\Gamma)} > \nu_{(H_2O^0-H_2O^0)} \quad (1)$$

Где H_2O^0 - молекула воды в объеме, H_2O^Γ - вода в гидратной оболочке иона. Другими словами, время осадкой жизни молекулы воды у иона больше чем в объеме

$$\tau_{H_2O^\Gamma} < \tau_{H_2O^0} \quad (2)$$

А под ионом, стабилизирующим структуры воды, подразумевается ионы для которых выполняется условия:

$$\nu_{H_2O^0-H_2O^\Gamma} < \nu_{H_2O^0-H_2O^0} \quad (3)$$

и

$$\tau_{H_2O^\Gamma} > \tau_{H_2O^0} \quad (4)$$

Полученные нами результаты, свидетельствуют о том, что в нашем случае, имеет место условия (3) и (4). При введении солей в систему молекулы воды у анионов (у всех исследованных солей катионы одинаковые) обмениваются с молекулами "свободные воды" меньшей частотой чем свободные молекулы воды между собой, что в итоге приводит к структурированию воды в целом.

Все выше изложенное позволяет качественно объяснить полученные в данной работе результаты по влиянию добавок солей на характеристики фазовой диаграммы двухфазной системы ПЭГ-натриевая соль лимонной кислоты-вода |.

Таким образом, смещения бинодалей фазовой диаграммы в сторону начала координат, увеличение площади гетерогенной области диаграммы при введении исследованных солей (NaNO_3 , Na_2SO_4 , Na_2CO_3 , KCl , KBr , KJ , K_2SO_4), а также уменьшение суммарной концентрации фазообразующих компонентов в критической точке двухфазной системы с увеличением концентрации соли (на примере NaNO_3) однозначно свидетельствуют о том, что эти соли оказывает структурирующие действия на водную среду системы.

Необходимо подчеркнуть, что изменения характеристики водно-двуофазной системы, естественно, отражается на процесс распределению различных веществ в этих двухфазной системе. Для количественной характеристики различия сродства фаз к распределяемом веществу нами было изучено разделительная способность (n^*) двухфазной систему ПЭГ (6000)-натриевая соль лимонной кислоты-вода при $T= 298,15 \text{ K}$ в отсутствии и присутствии различных солевых добавок. Полученные данные представлены в таблице 2. Разделительная способность системы определялась по методу предложенные в работу |6|.

Таблица 1. Разделительная способность двухфазной системы ПЭГ – натриевая соль лимонной кислоты – вода в присутствии некоторых солей

Систем	n^*
ПЭГ-натриевая соль лимонной кислоты-вода (ПЭГ- $\text{C}_6\text{H}_5\text{O}_7\text{Na}_3\text{-H}_2\text{O}$)	9,3
ПЭГ- $\text{C}_6\text{H}_5\text{O}_7\text{Na}_3\text{-H}_2\text{O} + \text{NaNO}_3$ (4,67 mol/l)	12,6
ПЭГ- $\text{C}_6\text{H}_5\text{O}_7\text{Na}_3\text{-H}_2\text{O} + \text{Na}_2\text{CO}_3$ (3,76 mol/l)	13,5
ПЭГ- $\text{C}_6\text{H}_5\text{O}_7\text{Na}_3\text{-H}_2\text{O} + \text{Na}_2\text{SO}_4$ (2,36 mol/l)	14,6
ПЭГ- $\text{C}_6\text{H}_5\text{O}_7\text{Na}_3\text{-H}_2\text{O} + \text{Na}_2\text{SO}_4$ (1,79 mol/l)	15,42
ПЭГ- $\text{C}_6\text{H}_5\text{O}_7\text{Na}_3\text{-H}_2\text{O} + \text{KCl}$ (5,5mol/l)	7,19
ПЭГ- $\text{C}_6\text{H}_5\text{O}_7\text{Na}_3\text{-H}_2\text{O} + \text{KBr}$ (3,53 mol/l)	6,98
ПЭГ- $\text{C}_6\text{H}_5\text{O}_7\text{Na}_3\text{-H}_2\text{O} + \text{KJ}$ (1,04mol/l)	10,6
ПЭГ- $\text{C}_6\text{H}_5\text{O}_7\text{Na}_3\text{-H}_2\text{O} + \text{K}_2\text{SO}_4$ (0,47mol/l)	14,35

Полученные результаты показывает что некоторые соли увеличивают величину разделительной способности что связано увеличение различия свойствах фаз а некоторые соли уменьшает n^* что связано с приближением свойств системы друг-другу

ЛИТЕРАТУРА

1. Альбертсон П. Разделение клеточных частиц и макромолекул. – М: Мир, 1974, 381 с.
2. Masimov E., İsmailov E., Odzhaqverdiyeva S., Complexation of polyethylene-glycol with the sodium salts of citric and succinic acids in the aqueous solutions. Studies by dynamic light scattering and uv/vis spectrophotometry Journal of Advances in Chemistry V.11, No 8, June 25, p.3866-3872
3. Albertson P.A., Biochim.Biophys.Acta.1958,27,N2.p.378-394
4. Zaslavsky B.Yu. и другие. Colloid Polymer Sci.1986, v. 264, p.1066-1071
5. Заславский Б.Ю. и др., ВМС, 1987, Т.296, N2, c.98-101
6. Zaslavsky B.Yu, Masimov E.A, Methods of the Analysis of the relative Hydrophobisity Biological solutes / topics current chemstry.-1988,-146,-P.171-202.
7. Journal of BAKU ENGINEERING UNIVERSITY, 2018, V2, N.2,, p.71-76
8. Масимов Э.А., Гасанов А.А., Гасанова Х.Т.» "STRUCTURAL TEMPERATURE" AND FREE ENERGY OF ACTIVATION OF VISCOUS FLOW OF AQUEOUS SOLUTIONS" Международный журнал прикладных и фундаментальных исследований, N4(1), 2015, с.40-44
9. Самойлов О.Я. Структура водных растворов электролитов М, Изд.АН СССР ст.15-18, 1967
10. Заславский Б.Ю, Масимов Э.А., и др. 1986, Т288, N1

UDC 532.73PACS:77.22.Ej, 64.75 Bc, 31.70.Dk, 61.70 Og

THE INFLUENCE OF ETHYLENE GLYCOL AND GLYCERIN TO THE FORMATION OF AQUEOUS BIPHASIC SYSTEM POLYETHYLENE GLICOL-SODIUM CITRATE-WATER

SHAHBAZOVA GUNEL MUGADDAS

Baku State University,

Baku, Azerbaijan

*Shahbazova.gunel@mail.ru***ABSTRACT**

In this work aqueous two-phase systems consisting of polyethylene glycol-sodium salt of citric acid and water have been studied. Experimental phase diagrams and the influence of ethylene glycol, glycerin to the phase diagram are presented. As a result if the system includes ethylene glycol and glycerin the binodal curve is splintered to top of coordinate, in other words, the separation of phases process occur at high concentration of polymers which formed phases. This means that ethylene glycol and glycerin acts as a factor that destroys the structure of water, breaking the hydrogen bonds between water molecules. As a result, the number of free water molecules increases, the phase-forming components are easier to dissolve, and the phase separation occurs at higher concentrations of the components.

Keywords: aqueous two phase systems, binodal curve, sodium citrate, ethylene glycol, glycerin

ВЛИЯНИЕ ЭТИЛЕНГЛИКОЛЯ И ГЛИЦЕРИНА НА ФОРМИРОВАНИЕ ВОДНОЙ ДВУХФАЗНОЙ СИСТЕМЫ ПОЛИЭТИЛЕНГЛИКОЛЬ- ЦИТРАТ НАТРИЯ -ВОДА

РЕЗЮМЕ

В данной работе были изучены водные двухфазные системы, состоящие из полиэтиленгликоль-натриевой соли лимонной кислоты и воды. Приведены экспериментальные фазовые диаграммы и влияние этиленгликоля, глицерина на фазовую диаграмму. В результате, если в систему входят этиленгликоль и глицерин, бинодальная кривая расщепляется до вершины координаты, другими словами, процесс разделения фаз происходит при высокой концентрации полимеров, образующих фазы. Это означает, что этиленгликоль и глицерин действуют как фактор, разрушающий структуру воды, разрывая водородные связи между молекулами воды. В результате количество свободных молекул воды увеличивается, фазообразующие компоненты легче растворяются, и фазовое разделение происходит при более высоких концентрациях компонентов.

Ключевые слова:водные двухфазные системы, бинодальная кривая, цитрат натрия, этиленгликоль, глицерин

PEQ-LIMONTURŞUSUNUN NATRİUM DUZU-SU İKİFAZALI SİSTEMİNİN ƏMƏLƏGƏLMƏSİNƏ ETİLENQLİKOL VƏ QLİSERİNİN TƏSİRİ

XÜLASƏ

Təqdim olunan işdə PEQ-limon turşusunun sodium duzu-su ikifazalı sisteminə baxılmışdır. Bu sistemin təcrübə əyri və bu sistemin əmələgəlməsinə etilenqlikol və qliserinin təsirinə baxılmışdır. Göstərilmişdir ki, etilenqlikol və qliserinin təsirilə PEQ-limon turşusunun sodium duzu-su sisteminin hal diaqramının binodallı heterogen oblast istiqamətinə tərəf sürüşür, başqa sözlə fazalara ayrılma komponentlərin daha böyük konsentrasiyalarında baş verir. Bu o deməkdir ki, etilenqlikol və qliserin su molekülləri arasındaki hidrogen rabitələrini qıraraq, suyun strukturunu daşıdan faktor kimi çıxış edir. Nəticədə sərbəst su molekullarının sayı artır, faza əmələ gətirən komponentlərin həllolması asanlaşır və fazalara ayrılma komponentlərin daha böyük konsentrasiyalarında baş verir.

Açar sözlər: sulu ikifazalı sistemlər, binodal əyri, limon turşusunun sodium duzu, etilenqlikol, qliserin.

INTRODUCTION

Aqueous two phase systems (ATPS) are aqueous solutions of a combination of two incompatible polymer or a polymer and a salt that separate into two phases when their concentration surpasses a certain threshold value [2]. One phase is rich in one polymer, and the second phase is rich in the other polymer as (or salt) with water as a solvent in both phases. ATPSs consist of two immiscible aqueous phases and have traditionally been used for the separation and purification of biological material such as proteins or cells [1].

Aqueous two phase systems (ATPS) based on water-soluble polymers are highly useful tools for extraction and purification of biomolecules [4-8].

Generally, the application of two-phase aqueous systems once a time move to the fore and the fundamental scientific investigation of these systems are relatively delayed. So that, formation mechanism of the two-phase aqueous polymer systems, influence of external factors to physical-chemical properties of them, the separation of some substances in these systems are explained in literature opposite ideas. Some writers were suggested solvent role of components. They claimed that if two polymer give two-phase systems in any solvent, then this incident must be observed in other solvents. In recent times, E.Masimov, Zaslavsky and others were suggested hypothesis that the formation of two-phase aqueous polymer systems, water has a key role in scientific investigation and they were confirmed with experimental facts.

As is known, water is organize most of the living world, and it is here play not only solvent role, but also biological active medium role. So that, the biological activity and functionality of high-molecular compounds, their structure and conformation in water environment, formed as a result of the interaction them with water. These interactions are widely investigated with different methods (such as scattering of light, IR, EPR, NMR spectroscopy and etc.). Water in contain base part of living organism and high-molecular compound and metabolism in organism is mainly performed by blood. For formation of simplest model of the processes in living organism which many-component, many-phase system, we can using two-phase polymer-polymer-water systems.

So these notes that allows us to the investigation of two-phase aqueous polymer systems have both fundamental and great practical importance.

MATERIALS AND METHODS

In this study using PEG with $M_n = 6000$ molecular weight which produced by "Panreac" firm of Spanish and "chemical cleaner" and "special cleaner" sodium citrate, glycerin, ethylene glycol.

Polyethylene glycol is a polyether compound derived from petroleum with many applications, from industrial manufacturing to medicine. PEG is also known as polyethylene oxide (PEO) or polyoxyethylene (POE), depending on its molecular weight. The structure of PEG is commonly expressed as $H-(O-CH_2-CH_2)_n-OH$.

Sodium citrate is the sodium salt of citric acid. This is a white, crystalline powder or white, granular crystals, weakly excreted in moist air, freely soluble in water, almost insoluble in alcohol. Like citric acid, it has a sour taste. From a medical point of view, it is used as an alkalinizing agent. It works by neutralizing excess acid in the blood and urine. Indicated for the treatment of metabolic acidosis

Researching of physical-chemical properties of two-phase systems in the phase formation dissolved in water two polymers or aqueous solution of any polymer which dissolved in water with inorganic salt to structuring water, studied mixtures in water of some organic salts. Knowing that, PEG give the two-phase system with some organic salts, including aqueous solution of sodium salt of citric acid ($C_6O_7H_5Na_3$).

According to the aqueous mixture of $C_6O_7H_5Na_3$ salt with PEG, to obtain two-phase system at certain concentration of components. As in the investigated two-phase aqueous polymer systems, at the same time existed phases of PEG- $C_6O_7H_5Na_3-H_2O$ systems they are keep both two components, they have different concentration in phases. At this time, the interaction between water and components play main role.

As is known, investigation of two-phase aqueous polymer systems are actual that is why the processes which these systems are can be accepted as the model of the processes which in living organisms. Really, the explore of biological substances separation between the phases which exist at the same time and differ from each other for hydrophobicity can help to explain metabolism mechanism that carried out with blood.

For illustrating aqueous biphasic polymer systems, it is conventional [1] to investigate the phase diagram-binodal curves, where the weight vs concentrations of the phase-forming components, the tie line, its length and angle of inclination, separation capacity, etc., are plotted along the coordinate axes. Fig. 1 shows the binodal curve of the PEG (6000)-sodium citrate/water, tie line, which is defined based on the method of least squares equation.

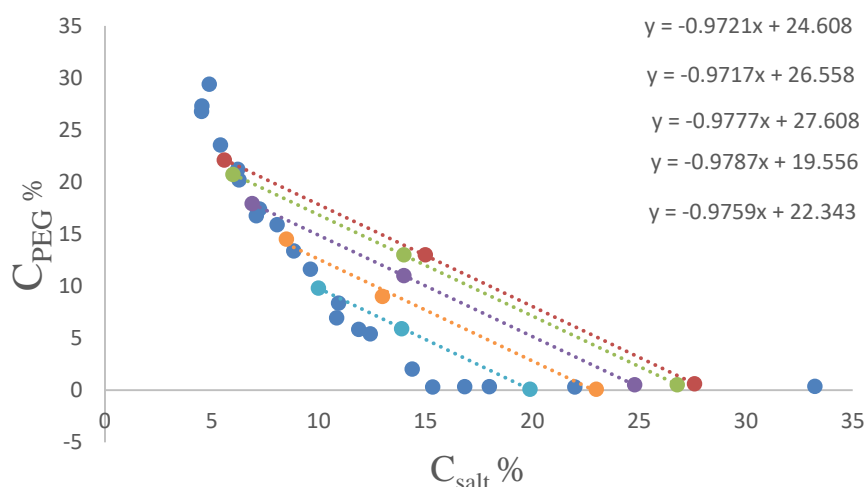


Fig. 1- Binodal curve and tie lines of the biphasic system PEG/sodium citrate -H₂O

The binodal curve and tendency angle of connecting (or tie) lines are taken as the main characteristic of aqueous two-phase systems.

Then investigated the influence of ethylene glycol and glycerin to the phase diagrams of aqueous biphasic system PEG-sodium citrate-water.

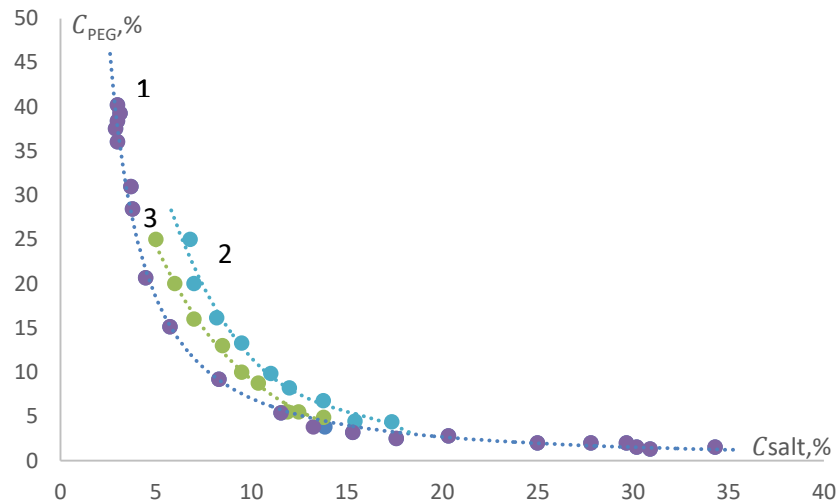


Fig. 2. Influence of polyhydric alcohols on the binodal curve of the two-phase system PEG-C₆H₅O₇Na₃-H₂O

1-binodal without additive, 2-ethylene glycol, 3-glycerin

In Figure 2. given the binodal curve of ($M_n = 6000$) PEG with sodium salt of citric acid aqueous solution the two-phase system and influence some alcohols(ethylene glycol, glycerin) to binodal curve.

With the influence of ethylene glycol, glycerin to the system, obtained that binodal curve is slipped to top of coordinate at the high concentrations, two-phase systems are occur with higher concentration of components which formed phases.

CONCLUSION

The formation of two-phase system is observed in aqueous mixture of polyethylene glycol with citrate at thermodynamic equilibrium. Phase diagram of acquired two-phase system (binodal curve and tendency angle of connecting or tie line) is investigated.

The results show that, with the influence of ethylene glycol, glycerin to the system, obtained that binodal curve is slipped to top of coordinate at the high concentrations, two-phase systems are occur with higher concentration of components which formed phases. This means that ethylene glycol and glycerin acts as a factor that destroys the structure of water, breaking the hydrogen bonds between water molecules. As a result, the number of free water molecules increases, the phase-forming components are easier to dissolve, and the phase separation occurs at higher concentrations of the components

REFERENCES

1. ALBERTSSON, P. A. 1986. PARTITION OF CELL PARTICLES AND MACROMOLECULES, 3RD ED. JOHN WILEY & SONS, NEW YORK.
2. S.HARDT, T.HAHN. MICROFLUIDICS WITH AQUEOUS TWO-PHASE SYSTEMS.LAB CHIP 12(2012) 434-442
3. ALBERTSSON, P.-Å. PARTITION OF CELL PARTICLES AND MACROMOLECULES, 3RD ED.; WILEY: NEW YORK, NY, USA, 1986.
4. HATTI-KAUL, R. AQUEOUS TWO-PHASE SYSTEMS. METHODS BIOTECHNOL. 2000, 11, 5-10.
5. ZASLAVSKY, B.Y. AQUEOUS TWO-PHASE PARTITIONING: PHYSICAL CHEMISTRY AND BIOANALYTICAL APPLICATIONS; MARCEL DEKKER: NEW YORK, NY, USA, 1995.
6. JOHANSSON, H.-O., MAGALDI, F.M.; FEITOSA, E.; PESSOA JUNIOR, A. PROTEIN PARTITIONING IN POLY(ETHYLENE GLYCOL)/SODIUM POLYACRYLATE AQUEOUS TWO-PHASE SYSTEMS. J. CHROMATOGR. A 2008, 1178, 145-153.
7. JOHANSSON, H.-O.; ISHII, M.; MINAGUTI, M.; FEITOSA, E.; PENNA, T.C.V.; PESSOA JUNIOR, A. SEPARATION AND PARTITIONING OF GREEN FLUORESCENT PROTEIN FROM ESCHERICHIA COLI HOMOGENATE IN POLY(ETHYLENE GLYCOL)/SODIUM-POLY(ACRYLATE) AQUEOUS TWO-PHASE SYSTEMS. SEP. PURIF. TECHNOL. 2008, 62, 166-174.
8. SARAVANAN, S.; RAO, J.R.; NAIR, B.U.; RAMASAMI, T. AQUEOUS TWO-PHASE POLY(ETHYLENE GLYCOL)POLY(ACRYLIC ACID) SYSTEM FOR PROTEIN PARTITIONING: INFLUENCE OF MOLECULAR WEIGHT, PH AND TEMPERATURE. PROCESS BIOCHEM. 2008, 43, 905-911.
9. МАСИМОВ Э.А., ШАХБАЗОВА Г.М., БАГИРОВ ТАЛЕТДИН ОРУДЖГУЛУ Т.О., ОДЖАГВЕРДИЕВА С.Я. ВЛИЯНИЯ НЕКОТОРЫХ ОДНОАТОМНЫХ СПИРТОВ НА ФАЗОВУЮ ДИАГРАММУ ПЭГ-НАТРИЕВАЯ СОЛЬ ЛИМОННОЙ КИСЛОТЫ-ВОДА, МЕЖДУНАРОДНЫЙ ЖУРНАЛ ПРИКЛАДНЫХ И ФУНДАМЕНТАЛЬНЫХ ИССЛЕДОВАНИЙ. – 2017. – № 9 – С. 140-142

PACS: 73.43.Lp *Collective excitations*

UDC: 620.91

CONDUCTIVE EXTENDED STATES IN $\text{Bi}_2\text{Te}_3\langle\text{In}, \text{Cu}\rangle$.

GOJAYEV E.M.

Azerbaijan Technical University, Baku, Azerbaijan
geldar-04@mail.ru

GAHRAMANOV A.SH.

Baku State University, Baku Azerbaijan

GAHRAMANOV S.SH.

Institute of Physics named after G.M. Abdullayev ANAS, Baku
samir.gahramanov@gmail.com

GULMAMMADOV K.J.

Azerbaijan Technical University, Baku, Azerbaijan
kamal.gul@mail.ru

MAMEDOVA S.I.

Azerbaijan Technical University, Baku
suraya.aztu@mail.ru

ABSTRACT

In this paper presents the results of a study of the temperature dependences of electrical conductivity and Hall coefficient. The Hall mobility was determined as the concentration of free carriers doped with Cu atoms - 0.05 wt% and In-01 wt% and of the stimulated magnetic field of Bi_2Te_3 crystals in the temperature range. Studies were conducted in the temperature range of 77-300, K. An analysis of the results showed that the formation of new covalent bonds through the long-range orbitals of large atoms $\text{Bi}_2\text{Te}_3\langle\text{In}, \text{Cu}\rangle$ creates binding states. The anharmonicity of the bonds and the membrane effect contribute to the overlapping of electronic functions between the layered elements, this leads to the formation of extended states, which in turn leads to an increase in the concentration of charge carriers, and conductivity. Changes in the interatomic distances in the crystal, coupled with the centers of disorder, enhance the effect of delocalization. A weak magnetic field also leads to the formation of extended states through charge delocalization during spin orientation of bonds.

Keywords: $\text{Bi}_2\text{Te}_3\langle\text{In}, \text{Cu}\rangle$, electrical conductivity, Hall coefficient, negative magnetic resistance, magnetic field, kinetic parameters.

ПРОВОДЯЩИЕ ПРОТЯЖЕННЫЕ СОСТОЯНИЯ В $\text{Bi}_2\text{Te}_3\langle\text{In}, \text{Cu}\rangle$.

РЕЗЮМЕ

В работе изложены результаты исследования температурных зависимостей удельной электропроводности, коэффициента Холла. Определены Холловская подвижность концентрация свободных носителей легированные атомами Cu – 0.05 вес% и In-01 вес% и стимулированных магнитного поля кристаллов Bi_2Te_3 в температурном интервале. Исследования проводились в температурном интервале 77-300, К. Анализом полученных результатов показано, что формирование новых ковалентных связей через дальнодействующие орбитали крупных атомов $\text{Bi}_2\text{Te}_3\langle\text{In}, \text{Cu}\rangle$ создает связывающие состояния. Ангармоничность связей и мембранный эффект способствуют перекрытию электронных функций между слоевыми элементами, это приводит к образованию протяженных состояний, что в свою очередь приводит к увеличению концентрации носителей заряда, и проводимости. Изменения межатомных расстояний в кристалле в купе с центрами

беспорядка усиливают эффект делокализации. Слабое магнитное поле также приводит к образованию протяженных состояний посредством делокализации заряда при спиновом ориентировании связей.

Ключевые слова: Bi₂Te₃<In,Cu>, электропроводность, коэффициент Холла, отрицательное магнитное сопротивление, магнитное поле, кинетические параметры.

Bi₂Te₃<In,Cu> BIRLƏŞMƏSINDƏ DAVAMLI KEÇİRİCİLİK HALI

XÜLASƏ

İşdə Cu – 0.05 çəki% və In-01 çəki % atomları ilə aşqarlanmış və maqnit sahəsi ilə stimullaşdırılmış Bi₂Te₃ kristallarının xüsusi elektrik keçiriciliklərinin, Holl əmsalının temperatur asılılıqları tədqiq edilmişdir. Sərbəst yükdaşıyıcıların Holl yüksüklükleri və konsentrasiyaları təyin edilmişdir. Tədqiqatlar 77-300, K temperatur intervalında aparılmışdır. Alınmış nəticələrin təhlili göstərmişdir ki, rəbitələrin anharmonikiyi və membran effekti təbəqə elektronları arasında elektron funksiyalarının kəsişmələrinə səbəb olur ki, bu da öz növbəsində uzunmüddətli halların əmələ gəlməsinə, nəticədə sərbəst yükdaşıyıcıların sayının və keçiriciliyin artmasına gətirir. Kristalda atomlararası məsafənin dəyişməsi nizamsızlıqla birləşdirilmiş delokallaşma effektini gücləndirir. Sabit maqnit sahəsi də həmçinin davamlı halların əmələ gəlməsinə rəbitələrin spin nizamlanması nəticəsində delokallaşmaya səbəb olur.

Açar sözlər: Bi₂Te₃ <In, Cu>, elektrik keçiriciliyi, Holl əmsali, mənfi maqnit müqaviməti, maqnit sahəsi, kinetik parametrlər.

Bismuth tellurides are layered structures, the crystalline matrix ...-Te⁽¹⁾-Bi-Te⁽²⁾-Bi-Te⁽¹⁾-...of which consists of layers separated by weak interactions. On the state of quintet layers of the crystal lattice is also affected by processes occurring in the interlayer space, which directly affect the redistribution of electron density and changes in the phonon subsystem. It is known that in layered crystals a part of superstoichiometric excess and impurities is formed in the interlayer space. A shift of the charge density deeper into the layer during broadening of the van der Waals gap [1, p.109], as well as an increase in the number of electrons from donor impurities, can lead to mutual repulsion of lone electron pairs in the Bi-Te⁽²⁾bond and to a change in the valence angle. Due to this charge displacement [2, p.233], a greater splitting of various types of molecular orbitals occurs, and non-binding orbitals are involved in the formation of covalent orbitals. Bi orbitals are combined with Te orbitals, with the formation of new binding orbitals instead of the original non-bonding orbitals, i.e. the bond takes on a metastable ion-covalent form. In the hybridization of bonds between Te⁽²⁾ and bismuth atoms, the initial system overlaps with the p-orbit of Te⁽²⁾ and the unshared bismuth electron pair transforms into conjugated system, accompanied by a redistribution of electron density.

The inhomogeneous distribution of electron density on the lattice centers on both sides of Bi, caused by a change in the valence state and leading to polarization of the electron system, can lead to the appearance of static and dynamic waves of charge's density. For waves of charge density, mixing of the binding orbital with its loosening is inherent; energetically, the binding and loosening levels are located symmetrically with respect to the Fermi level. A cycle consisting of 75K, at which fluctuations of the lattice parameter of Bi₂Te₃ crystals doped with Cu and In impurities occurs, is ~ 0.0065eV [3, p.315]. Approximately the same energy value is observed during fluctuations of kinetic parameters. The temperature behavior of these parameters apparently also shows a partial contribution to the change in the binding and loosening bonds, depending on the fluctuations of states corresponding to them near the Fermi level. This is accompanied by a change in the types of charge ordering, as well as changes in the formation of bonds and changes in the parameters of the crystal lattice. As can be seen, the temperature changes the energy state of the bonds, which, changing orientation, lead to compression and

decompression of the crystal in the direction of the "C" axis. A change in valence bonds leads to a change in charge ordering and, possibly, to its polarization as in the case of superconductivity in $\text{Bi}_2\text{Se}_3\text{Cu}$ [4, p.5,5,p. 3].

The redistribution of electron density may be accompanied by the formation of extended states conducting along long-range hybrid orbitals of heavy elements. The conducting extended states are akin to a long molecule, i.e. at a certain energy, a tunnel bond through atoms of heavy elements forms a weak chemical bond, because the interaction energy of the extreme electrons with the nucleus is weak, and a potentially forming new bond is also weak. Resonance or hybridization of bonds leads to the appearance of extended states, and an increase or decrease in energy relative to the level of the resonance state leads to the destruction of extended states and the absence of tunneling. According to the results of studying the kinetic parameters of Bi_2Te_3 crystals doped with Cu-0.05 wt% and In-0.1 wt% impurities obtained by vertical directional crystallization, shunting through extended states had activation peaks at 100K and 150K. Stimulation of these states by a weak magnetic field and their destruction at strong fields were observed: negative magnetoresistance NMR up to 10 kOe. An increase in temperature during magneto-field exposure led to an increase in the NMR from 100K to 170K, then the NMR sharply faded away, i.e. the effect of shunting over an extended conducting state was blocked. The destruction of the resonance bond leads to a return to the previous model of the distribution of bonds in the molecule and, accordingly, the electron density in the quintet. With the exception of the main, largest feature, extrema in the temperature dependences of the Hall coefficient (Fig. 1) and electrical conductivity (Fig. 2) as well as the concentration (Fig. 3) and carrier mobility (Fig. 4) in the region of 77-170K are possible from - due to an increase in the electronic component, during the transition of localized electrons from filled levels to unfilled with increasing temperature. The flow of electron density over the Bi-Te⁽²⁾ bond, which enhances the ionicity of the bond, shortens the interatomic distance, and an increase in the concentration of free carriers appears on the conductivity. An indirect confirmation of this is the negative magnetoresistance NMR at 100-170K (Fig. 5).

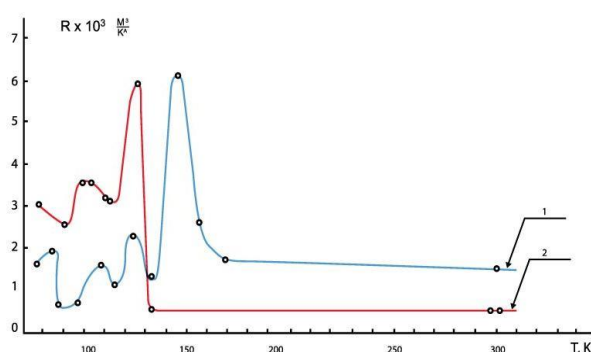


Fig. 1. Temperature dependences of the Hall coefficient $-R$ of $\text{Bi}_2\text{Te}_3\text{In,Cu}$ >sample with directions of experiment: 1 - $H \parallel C \perp J$; 2 - $H \perp C \perp J$

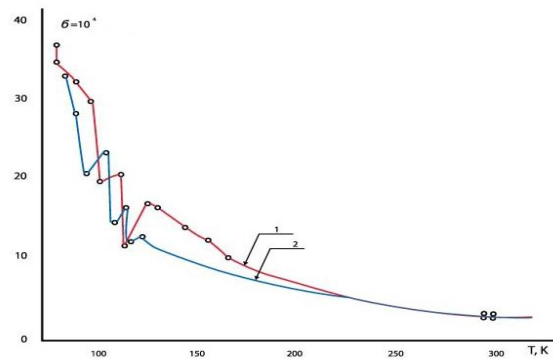


Fig. 2. Conductivity temperature dependences of $\text{Bi}_2\text{Te}_3\text{In,Cu}$ >sample with directions of the experiment: 1 - $H \parallel C \perp J$; 2 - $H \perp C \perp J$

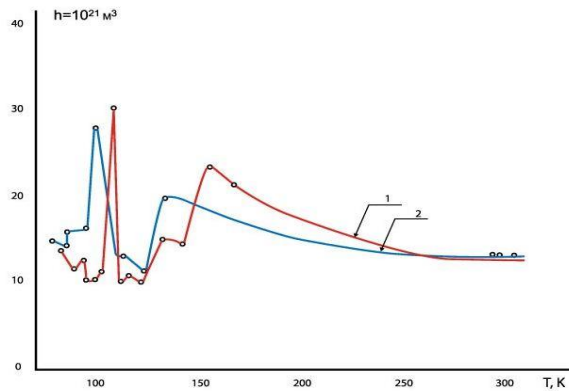


Fig. 3. Temperature dependences of the Hall charge carriers concentration - n $\text{Bi}_2\text{Te}_3\text{<} \text{In}, \text{Cu} \text{>}$ for experimental directions: 1- $H \parallel C \perp J$; 2- $H \perp C \perp J$

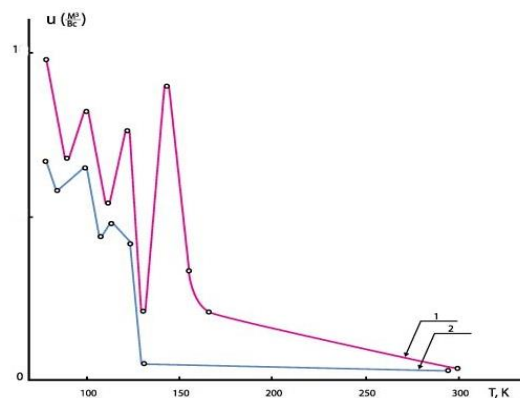


Fig. 4. Temperature dependences of the mobility - u $\text{Bi}_2\text{Te}_3\text{<} \text{In}, \text{Cu} \text{>}$ for experimental directions: 1- $H \parallel C \perp J$; 2- $H \perp C \perp J$

The anharmonicity of bonds, which was pointed out by other authors as the cause of bond deviation at T100K-150K, is a consequence of the flow of electron density over the bond. The temperature dependences of the elastic constants in layered crystals revealed a tendency for a more rapid change in the interlayer elastic constants as compared to the intralayer ones [6, p. 667.].

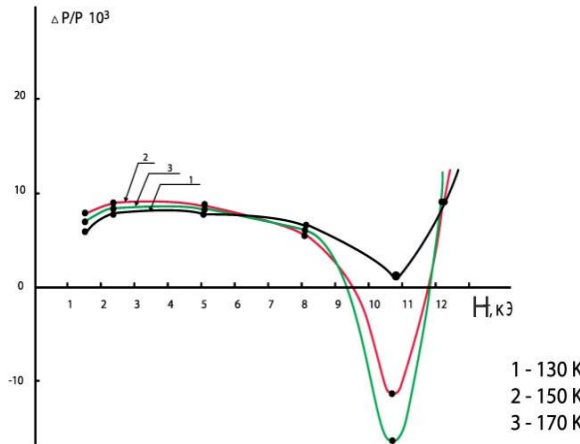


Fig. 5. Dependences of the transverse magnetoresistance $\Delta P/P$ from the magnetic field H for the $\text{Bi}_2\text{Te}_3\text{<} \text{In}, \text{Cu} \text{>}$ sample

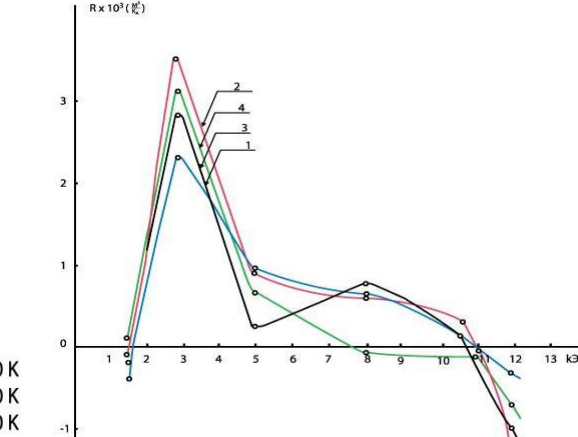


Fig. 6. Dependence of the Hall coefficient - R on the magnetic field for a $\text{Bi}_2\text{Te}_3\text{<} \text{In}, \text{Cu} \text{>}$ sample at temperature: 1 – 110K; 2 – 120K; 3 – 150K; 4 – 170K

It is noted that a change in the values of elastic constants with temperature is an anharmonic phenomenon and occurs due to two processes: phonon-phonon interaction and lattice deformation due to thermal expansion. The anharmonicity of the bonding forces between the layers is substantially greater than the anharmonicity of the intralayer forces. Moreover, the contribution of thermal expansion to this change is much higher for the "interlayer" elastic constant than for the "intralayer" [7, p. 293]. Intralayer (within the five-layer quintet packet) bonds in bismuth chalcogenides are sensitive to changes in the magnitude of the interlayer interaction.

A weak magnetic field apparently leads to the delocalization of precisely electrons on the metastable configuration of orbitals near defective centers. A surge in kinetic parameters is possibly associated with delocalization during the formation of extended bonds, the

anharmonicity of the bonds and the membrane effect contribute to the overlap of the orbitals between the layer elements. The overlapping of the electronic functions of the layers leads to the formation of extended states; this, in turn, leads to an increase in the concentration of charge carriers, conductivity, etc. A weak magnetic field also leads to the formation of extended states by delocalization of the charge with spin orientation of the bonds.

REFERENCES:

1. T.V. Menshchikova, S.V. Eremeev, E.V. Chulkov. On the origin of two-dimensional electron gas states at the surface of topological insulators. *JETP Letters*. 2011, Vol.94, No.2, pp 106-111.
2. M. G. Vergniory, T. V. Menshikova, S. V. Eremeev, E. V. Chulkov, Ab initio study of 2DEG at the surface of topological insulator Bi₂Te₃. *Pis'ma v Zh. Eksp. Teoret. Fiz.*, Vol. 95, Iss. 4, pp 230–235, 2012.
3. Gahramanov S.Sh., Mehdiyev T.R., Huseynov G.G., Amirov A.S. Features of thermal expansion of doped bismuth telluride. *Interstate Conference "Thermoelectrics and Their Applications - 2014"* November 18-19, , A.F. Ioffe Institute of Physics and Technology St. Petersburg, Russia, pp. 313-318, 2014
4. Y.S.Hor, A.J.Williams, J.G.Checkelsky, P.Roushan, J.Seo, Q.Xu, H.W.Zandbergen, A.Yazdani, N.P. Ong, R.J.Cava. Superconductivity in Cu_xBi₂Se₃ and its implications for pairing in the undoped topological insulator. *Phys. Rev. Lett.* 104, 057001, 1-9, 2010.
5. Y.Ando, K.Segawa, S.Sasaki, M.Kriener. Experimental studies of the topological superconductor Cu_xBi₂Se₃. *Journal of Physics: Conference Series* 449, 012033, 1-5, 2013.
6. N. A. Abdullaev. Elastic properties of layered crystals. *Physics of the Solid State*, Vol. 48, No. 4, pp. 663–669, 2006. DOI: 10.1134/S1063783406040081
7. Z.I. Badalova, N.A. Abdullayev, G.H. Azhdarov, Kh.V. Aliguliyeva, S.Sh. Gahramanov, S.A. Nemov, N.T. Mamedov. Anharmonicity of lattice vibrations in Bi₂Se₃ single crystals. *Semiconductors*, Vol. 53, Iss.3, pp 291–295, 2019 <https://doi.org/10.1134/S1063782619030035>

PACS: 68.35.bm -Polymers, organics71.20.Rv Polymers and organic compoundsIOT: UDC: 620.91

INFLUENCE OF THE SEASHELL ON THE MECHANICAL AND ELECTRICAL STRENGTH OF HIGH PRESSURE POLYETHYLENE

E.M. GOJAYEV, Sh.A.ZEYNALOV, K.J.GULMAMMADOV, R.S. RAGIMOV, N.F. MEMMEDZADE

Azerbaijan Technical University

geldar-04@aztu.edu.az

ABSTRACT

In the paper given the results of a study of the mechanical and electrical strength of bio-composites based polyethylene low density modified with seashell, LDPE + x vol.% Seashell, where x = 0; 3; 5; 7; 10; 15 depending on the volumetric content of the bio-filler-seashell, on the electric field strength and on the magnitude of the mechanical deformation.

Samples obtained by hot pressing. The polymer + shell mixture is heated to the polymer melting point; at the same temperature, it is aged under pressure of 15 MPa for 15 minutes and cooled in an ice-water mixture.

It was revealed that for small values of the filler 3 vol.% Shell, the mechanical strength of the bio-composites increases, when the content reaches its maximum value. The maximum value of the electric strength of the films of bio-composites is achieved when 5 vol.% Shell are introduced into its composition. The increase in the electrical and mechanical strengths of the LDPE film with the introduction of the optimal amount of additive can be explained on the basis of changes in the physical structure of LDPE.

Key words: mechanical and electric strength, seashell, bio-composites, mechanical deformation, electric field strength.

ВЛИЯНИЕ РАКУШКИ НА МЕХАНИЧЕСКУЮ И ЭЛЕКТРИЧЕСКУЮ ПРОЧНОСТЬ ПОЛИЭТИЛЕНА ВЫСОКОГО ДАВЛЕНИЯ

АННОТАЦИЯ

В статье приведены результаты исследования механической и электрической прочности биокомпозитов на основе полиэтилена низкой плотности, модифицированного морской ракушкой(Р), ПЭВД + x об.% Р, в зависимости от объемного содержания бионаполнителя-морской ракушки, напряженности электрического поля и величины механической деформации, где x = 0; 3; 5; 7; 10; 15.

Образцы получены методом горячим прессованием. Смесь полимер+ракушка нагревают до температуры плавления полимера; при той же температуре его выдерживают под давлением 15 МПа в течение 15 минут и охлаждают в ледяной воде.

Выявлено, что при малых содержаниях наполнителя 3 об.% Р механическая прочность биокомпозитов увеличивается, достигает максимального значения. Максимальное значение электрической прочности пленок биокомпозитов достигается при введении в их состав 5 об.% Р. Увеличение электрической и механической прочности пленки ПЭВД при введении оптимального количества добавки можно объяснить изменениями в физической структуре ПЭВД.

Ключевые слова: механическая и электрическая прочность, морская раковина, биокомпозиты, механическая деформация, напряженность электрического поля.

BALIQQLAGİNİN AŞAĞI SIXLIQLI POLİETILENİN MEXANİK VƏ ELEKTRİK MÖHKƏMLİKLƏRİNƏ TƏSİRİ

XÜLASƏ

Məqalədə aşağı sıxlıqlı polietilen (ASPE) əsasında balıq qulağı (BQ) ilə modifikasiya olunmuş, bio-kompozitlərin ASPE + x həcm.% BQ (x = 0; 3; 5; 7; 10; 15) mexaniki və elektrik möhkəmlilikləri balıqqlağının doldurucusunun həcmi miqdarından və elektrik sahəsinin intensivliyindən və mexaniki deformasiyanın qiymətindən asılı olaraq tədqiqinin nticələri verilmişdir.

Nümunələr istipresləmə üsulu ilə alınmışdır. Polimer -balıqqulağı qarışığı əvvəlcə polimerin ərimə nöqtəsinə qədər qızdırılır; bu temperaturda 15 MPa təzyiq altında 15 dəqiqə müddətində saxlanılır və əriməkdə olan buz vasitəsilə soyudulur.

Tədqiqatlar nəticəsində müəyyən edilmişdir ki, doldurucunun 3 həcm% BQ qiymətində mexaniki möhkəmlik maksimal qiymətini alır. Biokompozitlərin elektrik döyünlülüklerinin maksimal qiymətləri isə tərkibində 5 həcm% BQ olması halında müşahidə edilir. Doldurucunun optimal qiymətində ASPE – nin elektrik və mexaniki döyünlülüklerinin artması ASPE – nin fiziki quruluşunun dəyişməsi ilə izah oluna bilər.

Açar sözlər: mexaniki və elektrik gücü, dəniz qabığı, bio-kompozitlər, mexaniki deformasiya, elektrik sahəsinin gücü.

INTRODUCTION

The use of polymeric materials provides the opportunity to create a fundamentally new design and various types of products, helps to reduce their weight, operating and transportation costs, improve quality, physical and mechanical properties and appearance. It should be noted that the proportion of individual polymers among such materials is small. This is explained by the fact that for specific purposes, as a rule, polymers with a new set of properties are needed and it is preferable to solve this problem based on new materials with controlled properties. A convincing achievement to solve such problems is the creation of ordered heat-resistant, frost-resistant structural materials, as well as composite materials designed for use in harsh conditions [1-5].

The need to have any material with a specific set of properties led to the fact that when creating polymer compositions they were guided mainly by practical considerations [6-11].

For practical purposes, the most interesting is the determination of the electrical durability of the service life of polymer insulating materials and the effect on them of various modifying additives of various origins. Modifying additives leads to a change in many properties of polymers. In this case, the modified polymers change the mechanical tensile, bending and compression strengths of the respective elastic modulus, impact resistance, hardness, softening temperature and thermal conductivity. Depending on the origin and content of the fillers, the mechanical and electrical strengths of the composites can significantly change. [12-14]

We note that the introduction of additives into the polymer matrix has the following goals: modification of physical, mechanical, electrical properties: to prevent destruction from exposure to heat or ionizing radiation; material cost reduction; changes in color, transparency or other optical properties and appearance, improvement of technological properties. Therefore, the use of additives allows you to directionally adjust the properties of the final product. The effect of mechanical stress and additives on the change in the electrophysical properties of composite materials has been studied in many works [14, 15]. However, the change in the electrophysical properties of modified composite films in the presence of mechanical loading has not been studied enough.

The experimental technique

Samples obtained by hot pressing. The polymer + shell mixture is heated to the polymer melting point; at the same temperature, it is aged under pressure of 15 MPa for 15 minutes and cooled in an ice-water mixture.

Samples for testing the force dependence of mechanical durability and strength were cut out of the film in the form of a double blade, the length of the working part 10 mm wide 3 mm. Measurement of mechanical strength was carried out given in the work [15]. The installation for

measuring mechanical durability should ensure the fulfillment of two basic requirements: the effective tensile stress and temperature should not change during each test.

Measurement of the electrical durability of the composite film, the following electrode design was used [16]. The test sample was made in a rectangular shape with dimensions of 40x50 mm. During the test, the sample was between the electrodes. Before the test, the thickness of each sample was measured for 6-8 work places, after which the arithmetic mean value was found.

RESULTS AND DISCUSSION

The electric strength of the LDPE + Shell film depending on the amount of additives was determined on the basis of studying the kinetics of the development of electrical breakdown according to the developed technique.

The obtained experimental results are shown in Figures. 1 and 2. The introduction of an additive from a shell into the composition of LDPE leads to a significant change in its electrical durability (Fig. 1). As follows from the experimental data, in the case under consideration, when a certain amount of filler is introduced into the composition of LDPE, its electric strength increases. The maximum increase is observed for a biocomposite with a volumetric filler content of 7%. This means that by increasing the lifetime of the LDPE film with the introduction of the additive, it is possible to determine the optimal conditions for the modification of the electrophysical properties of LDPE to determine the effect of the composition of the added additive on the change in the electric strength of the LDPE film. The data are shown in Fig. 3. It can be seen that the introduction of a shell additive in LDPE also leads to a change in its electric strength [16,17], as the electric field strength increases, it linearly supplies the logarithm of electric durability, i.e. the well-known relation $\tau = B \exp(-\beta E)$ holds, where parameters B and β depend on the nature of the polymer and the test temperature. However, their numerical values turn out to be different. For a clearer picture of the development of electrical failure in a modified polymer, Fig.2 shows the dependence of the electric strength of the LDPE film on the weight percent of this additive under other identical conditions ($\tau = \text{const}$, $t = \text{const}$). The dependence $E_{pr} = f(C)$ is constructed according to the data used for the graph (Fig.2). As can be seen from Fig.4, the electric strength of the LDPE film reaches its maximum value when 5 vol% of a shell is introduced into its composition. As follows from the obtained results, when the optimal content of the proposed additive is introduced into the composition of LDPE, its electric strength increases from $12 \cdot 10^7$ to $17 \cdot 10^7$ V / m.

Indeed, as follows from the experimental data, the optimum content of additives of biological origin in the composition of LDPE in the detected positive effect is only 5 vol.% Seashell.

Changing the mechanical strength of polymer composites with fillers seashells, were shown in Fig. 3. As follows from Fig. 5 at low contents of the shell (0-3 vol.%) in the composition of LDPE, the mechanical strength increases reaching a maximum at an optimum filler content of 0-3 vol.% Shell, with a further increase in the volumetric amount of the filler monotonously decreases.

Thus, analyzing the experimental results, it can be assumed that the increase in the electrophysical properties of the LDPE film with the introduction of the optimal amount of additive used can be explained on the basis of changes in the physical structure of LDPE. At the same time, due to physical structure formation, heterogeneity in the mutual arrangement of macromolecules seems to decrease, as a result of which the conversion process and ionization processes in them are significantly slowed down.

It is important to note that the equation

$$\tau = \tau_0 \exp\left[\frac{(U_0 - \gamma\sigma)}{kT}\right]$$

expressing the temperature - time dependence of the mechanical strength of polymers indicates that the destruction of polymers under the action of mechanical load is a kinetically activation process that develops in time and is controlled by temperature and mechanical stress. It indicates that, firstly, the time factor is a fundamental characteristic of polymer strength, and secondly, the breakdown is nothing more than an activation process, the rate of which is determined by the frequency of thermal fluctuations by the ratio of the average energy of thermal motion and the value of the energy barrier reduced by the applied external mechanical stress [18].

CONCLUSION

Investigations of the electrical durability and mechanical strength of bio-composites LDPE + Shell have established the optimum values of seashell additives that correspond to their maximum. It was shown that an increase in the strength of biocomposites is observed at a low volumetric content of the bio-filler from the seashell.

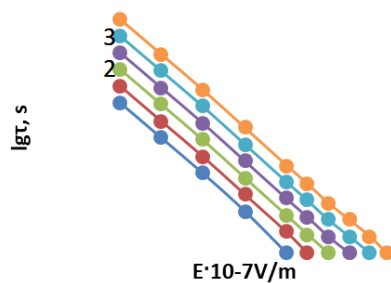


Figure. 1. Dependence of the electrical durability of LDPE biocomposites + x vol.% Seashell on the electric field strength. 1 - x = 0; 2 - x = 3; 3 - x = 5; 4 - x = 7; 5 - x = 10; 6 - x = 15.

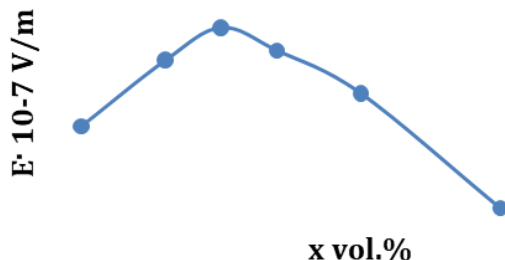


Figure. 2. Change in the electric strength of LDPE biocomposites + x vol.% Seashell from the volume content of the filler.

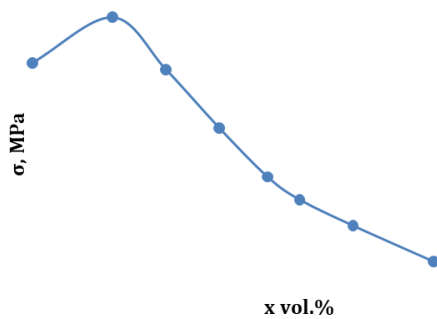


Figure. 3. The dependence of the mechanical strength of LDPE biocomposites + x vol.% Shell on the volumetric content of the filler.

REFERENCES

1. Plastics Used in Medical Devices Handbook of Polymer Applications in Medicine and Medical Devices, Plastics Design Library, p. 21-53, 2014.
2. Nurul, M.S.; Mariatti, M. Effect of hybrid nanofillers on the thermal, mechanical, and physical properties of polypropylene composites. *Polym. Bull.* 70, p.871-884, 2013.
3. Müller, M.T.; Krause, B.; Kretzschmar, B.; Jahn, I.; Pötschke, P. Thermal conductivity of hybrid filled HDPE nanocomposites. *AIP Conf. Proc.*, 1914, 030006, 2017.
4. Gojny, F.H.; Wichmann, M.H.G.; Fiedler, B.; Kinloch, I.A.; Bauhofer, W.; Windle, A.H.; Schulte, K. Evaluation and identification of electrical and thermal conduction mechanisms in carbon nanotube/epoxy composites. *Polymer*, 47, p. 2036–2045. 2006
5. H. Y. Atay, *Polymer Composites; Properties, Performance and Applications*, *Polymer science: research advances, practical applications and educational aspects* (A. Méndez-Vilas; A. Solano, Eds.) p.420-428, 2016.
6. T. L. Hanley, R. P. Burford, R. J. Fleming, and K. W. Barber, "A general review of polymeric insulation for use in HVDC cables," *IEEE Electrical Insulation Magazine*, vol. 19, Issue 1, p. 13–24, 2003.
7. S. Li, G. Yin, and J. Li, "Breakdown performance of low density polyethylene nanocomposites," in *Proceedings of the 10th IEEE International Conference on the Properties and Applications of Dielectric Materials (ICPADM '12)*, p.1-4, 2012.
8. K. Theodosiou, I. Vitellas, I. Gialas, and D. P. Agoris, "Polymer films degradation and breakdown in high voltage AC fields," *Journal of Electrical Engineering*, vol.55, p.225–231, 2004.
9. Olena Yakovenko, Ludmila Matzui, Ganna Danylova, Victor Zadorozhnii, Ludmila Vovchenko, Yulia Perets, and Oleksandra Lazarenko *Electrical Properties of Composite Materials with Electric Field-Assisted Alignment of Nanocarbon Fillers* *Nanoscale Res Lett*; 12: p.471. 2017.
10. Kristina Rojdev, Mary Jane E O'Rourke, Charles Hill, Steven Nutt, William Atwell *Radiation effects on composites for long-duration lunar habitats* , *Journal of Composite Materials* Vol. 48 issue 7, p.861-878, 2014
11. Berlin A.A. *Modern polymer composite materials*. - Soros Educational Journal. Issue 1, p. 57-65, 1995.
- P.-Y. Chen , A.Y.M. Lin , Y.-S. Lin , Y. Seki , A.G. Stokes , J. Peyras , E.A. Olevsky , M.A. Meyers, J. McKittrick, Structure and mechanical properties of selected biological materials, *Journal of the Mechanical Behavior Of Biomedical Materials*,1,p.208-226, 2008.
12. B. M. Primachenko, K. O. Strokin. *Study of the Mechanical Properties of Polymer Composite Material with Different Structures*, *Fibre Chemistry*, Vol. 50, Issue 4, p.368–372, 2018.
13. M. Oliviaaa,, A.A. Mifshella, L. Darmayantia, *Mechanical properties of seashell concrete*. *Procedia Engineering* 125, p.760-764, 2015.
14. K.Vignesh, K.Anbazhagan, E.Ashokkumar, R.Manikandan, A.Jayanth. *Experimental Analysis of Mechanical Properties of Sea Shell Particles- Polymer Matrix Composite*, *International Journal of Mechanical and Industrial Technology*, Vol. 3, Issue 1, pp.13-21, 2015.
15. State standard, R 56785-2015 *Polymer composites. Tensile test method for flat specimens*, 31p. (russia)
16. E.M.Gojayev, V.V.Salimova, P.F. Aliyeva // *Influence of fillers of biological origin and metal nanoparticles on the electrical properties of biocomposites*. *Eurasian Union of Scientists (ESU)* vol.62, Issue 5 part 5, p.9-13. 2019.(Russian)
17. V.G. Shevchenko *Fundamentals of the physics of polymer composite materials*. Moscow, 99p., 2010.
18. G.M. Bartenev, S.Ya. Frenkel *Physics of Polymers*. 1990, p. 433.

INSTRUCTIONS FOR AUTHORS

1. "The Baku Engineering University Journal-Physics" accepts original unpublished articles and reviews in the research field of the author.
2. Articles are accepted in English.
3. File format should be compatible with **Microsoft Word** and must be sent to the electronic mail (journal@beu.edu.az) of the Journal. The submitted article should follow the following format:
 - Article title, author's name and surname
 - The name of workplace
 - Mail address
 - Abstract and key words
4. The title of the article should be in each of the three languages of the abstract and should be centred on the page and in bold capitals before each summary.
5. **The abstract** should be written in **9 point** type size, between **100** and **150** words. The abstract should be written in the language of the text and in two more languages given above. The abstracts of the article written in each of the three languages should correspond to one another. The keywords should be written in two more languages besides the language of the article and should be at least three words.
6. **. UDC and PACS index** should be used in the article.
7. The article must consist of the followings:
 - Introduction
 - Research method and research
 - Discussion of research method and its results
 - In case the reference is in Russian it must be given in the Latin alphabet with the original language shown in brackets.
8. **Figures, pictures, graphics and tables** must be of publishing quality and inside the text. Figures, pictures and graphics should be captioned underneath, tables should be captioned above.
9. **References** should be given in square brackets in the text and listed according to the order inside the text at the end of the article. In order to cite the same reference twice or more, the appropriate pages should be given while keeping the numerical order. For example: [7, p.15].

Information about each of the given references should be full, clear and accurate. The bibliographic description of the reference should be cited according to its type (monograph, textbook, scientific research paper and etc.) While citing to scientific research articles, materials of symposiums, conferences and other popular scientific events, the name of the article, lecture or paper should be given.

Samples:

- a) **Article:** Demukhamedova S.D., Aliyeva İ.N., Godjayev N.M.. *Spatial and electronic structure of monomerrik and dimeric conapeetes of carnosine üith zinc*, Journal of structural Chemistry, Vol.51, No.5, p.824-832, 2010
- b) **Book:** Christie John Geankoplis. *Transport Processes and Separation Process Principles*. Fourth Edition, Prentice Hall, p.386-398, 2002
- c) **Conference paper:** Sadychov F.S., Aydin C., Ahmedov A.I.. Appligation of Information – Commu-nication Technologies in Science and education. II International Conference."Higher Twist Effects In Photon- Proton Collisions", Baki, 01-03 Noyabr, 2007, ss 384-391
References should be in 9-point type size.
10. The margins sizes of the page: - Top 2.8 cm. bottom 2.8 cm. left 2.5 cm, right 2.5 cm. The article main text should be written in Palatino Linotype 11 point type size single-spaced. Paragraph spacing should be 6 point.
11. The maximum number of pages for an article should not exceed 15 pages
12. The decision to publish a given article is made through the following procedures:
 - The article is sent to at least to experts.
 - The article is sent back to the author to make amendments upon the recommendations of referees.
 - After author makes amendments upon the recommendations of referees the article can be sent for the publication by the Editorial Board of the journal.

YAZI VƏ NƏŞR QAYDALARI

1. "Journal of Baku Engineering University" Fizika- əvvəller nəşr olunmamış orijinal əsərləri və müəllifin tədqiqat sahəsi üzrə yazılmış icmal məqalələri qəbul edir.
2. Məqalələr İngilis dilində qəbul edilir.
3. Yazilar Microsoft Word yazı programında, (journal@beu.edu.az) ünvanına göndərilməlidir. Göndərilən məqalələrdə aşağıdakılara nəzərə alınmalıdır:
 - Məqalənin başlığı, müəllifin adı, soyadı,
 - İş yeri,
 - Elektron ünvanı,
 - Xülasə və açar sözlər.
4. **Məqalədə başlıq hər xülasədən əvvəl** ortada, qara və böyük hərfə xülasələrin yazıldığı hər üç dildə olmalıdır.
5. **Xülasə** 100-150 söz aralığında olmaqla, 9 punto yazı tipi böyüklüyündə, məqalənin yazıldığı dildə və bundan əlavə yuxarıda göstərilən iki dildə olmalıdır. Məqalənin hər üç dildə yazılmış xülasəsi bir-birinin eyni olmalıdır. Açıq sözlər uyğun xülasələrin sonunda onun yazıldığı dildə verilməklə ən azı üç sözdən ibarət olmalıdır.
6. Məqalədə UOT və PACS kodları göstərilməlidir.
7. Məqalə aşağıdakılardan ibarət olmalıdır:
 - Giriş,
 - Tədqiqat metodu
 - Tədqiqat işinin müzakirəsi və onun nəticələri,
 - İstinad ədəbiyyatı rus dilində olduğu halda orjinal dili mötərzə içərisində göstərməklə yalnız Latin əlifbası ilə verilməlidir.
8. **Şəkil, rəsm, grafik və cədvəllər** çapda düzgün, aydın çıxacaq vəziyyətdə və mətn içərisində olmalıdır. Şəkil, rəsm və grafiklərin yazıları onların altında yazılmalıdır. Cədvəllərdə başlıq cədvəlin üstündə yazılmalıdır.
9. **Mənbələr** mətn içərisində kvadrat mötərizə daxilində göstərilməklə məqalənin sonunda mətn daxilindəki sıra ilə düzülməlidir. Eyni mənbəyə iki və daha çox istinad edildikdə əvvəlki sıra sayı saxlanmaqla müvafiq səhifələr göstərilməlidir. Məsələn: [7,səh.15].

Ədəbiyyat siyahısında verilən hər bir istinad haqqında məlumat tam və dəqiq olmalıdır. İstinad olunan mənbənin bibliografiya təsviri onun növündən (monoqrafiya, dərslik, elmi məqalə və s.) asılı olaraq verilməlidir. Elmi məqalələrə, simpozium, konfrans, və digər nüfuzlu elmi tədbirlərin materiallarına və ya tezislərinə istinad edərkən məqalənin, məruzənin və ya tezisin adı göstərilməlidir.

Nümunələr:

- a) **Məqalə:** Demukhamedova S.D., Aliyeva İ.N., Godjayev N.M.. *Spatial and electronic structure af monomeric and dimeric complexes of carnosine with zinc*, Journal of structural Chemistry, Vol.51, No.5, p.824-832, 2010
- b) **Kitab:** Christie ohn Geankoplis. *Transport Processes and Separation Process Principles*. Fourth Edition, Prentice Hall, 2002
- c) **Konfrans:** Sadychov F.S., Aydin C., Ahmedov A.İ.. Appligation of Information-Communication Technologies in Science and education. II International Conference. "Higher Twist Effects In Photon- Proton Collisions", Baki, 01-03 Noyabr, 2007, ss 384-391

Mənbələr 9 punto yazı tipi böyüklüyündə olmalıdır.

10. **Səhifə ölçüləri:** üstdən 2.8 sm, altdan 2.8 sm, soldan 2.5 sm və sağdan 2.5 sm olmalıdır. Mətn 11 punto yazı tipi böyüklüyündə, **Palatino Linotype** yazı tipi ilə və tək simvol aralığında yazılmalıdır. Paraqraflar arasında 6 punto yazı tipi aralığında məsafə olmalıdır.
11. Orijinal tədqiqat əsərlərinin tam mətni bir qayda olaraq 15 səhifədən artıq olmamalıdır.
12. Məqalənin nəşrə təqdimi aşağıdakı qaydada aparılır:
 - Hər məqallə ən azı iki ekspertə göndərilir.
 - Ekspertlərin tövsiyələrini nəzərə almaq üçün məqalə müəllifə göndərilir.
 - Məqalə, ekspertlərin tənqidini qeydləri müəllif tərəfindən nəzərə alındıqdan sonra Jurnalın Redaksiya Heyəti tərəfindən çapa təqdim oluna bilər.

YAZIM KURALLARI

1. "Journal of Baku Engineering University-Physics" önceler yayımlanmamış orijinal çalışmaları ve yazarın kendi araştırma alanının-da yazılmış derleme makaleleri kabul etmektedir.
2. Makaleler İngilizce kabul edilir.
3. Makaleler Microsoft Word yazı programında, (journal@beu.edu.az) adresine gönderilmelidir. Gönderilen makalelerde şunlar dikkate alınmalıdır:
 - Makalenin başlığı, yazarın adı, soyadı,
 - İş yeri,
 - E-posta adresi,
 - Özeti ve anahtar kelimeler.
4. **Özet** 100-150 kelime arasında olup 9 font büyüğünde, makalenin yazıldığı dilde ve yukarıda belirtilen iki dilde olmalıdır. Makalenin her üç dilde yazılmış özeti birbirinin aynı olmalıdır. Anahtar kelimeler uygun özeti sonunda onun yazıldığı dilde verilmekle en az üç sözcükten oluşmalıdır.
5. Makalede UOT ve PACS tipli kodlar gösterilmelidir.
6. Makale şunlardan oluşmalıdır:
 - Giriş,
 - Araştırma yöntemi
 - Araştırma
 - Tartışma ve sonuçlar,
 - İstinat Edebiyatı Rusça olduğu halde orjinal dili parantez içerisinde göstermekle yalnız Latin alfabesi ile verilmelidir.
7. **Şekil, Resim, Grafik ve Tablolar** baskında düzgün çıkacak nitelikte ve metin içerisinde olmalıdır. Şekil, Resim ve grafiklerin yazıları onların alt kısmında yer almalıdır. Tablolarda ise başlık, tablonun üst kısmında bulunmalıdır.
8. **Kullanılan kaynaklar**, metin dâhilinde köşeli parantez içerisinde numaralandırılmalı, aynı sırayla metin sonunda gösterilmelidir. Aynı kaynaklara tekrar başvurulduğunda sıra muhafaza edilmelidir. Örneğin: [7, seh.15]. Referans verilen her bir kaynağın künnesi tam ve kesin olmalıdır. Referans gösterilen kaynağın türü de eserin türüne (monografi, derslik, ilmî makale vs.) uygun olarak verilmelidir. İlmi makalelere, sempozyum, ve konferanslara müracaat ederken makalenin, bildirinin veya bildiri özetlerinin adı da gösterilmelidir.

Örnekler:

- a) **Makale:** Demukhamedova S.D., Aliyeva İ.N., Godjayev N.M.. *Spatial and Electronic Structure of Monomerik and Dimeric Conapeetes of Carnosine Üith Zinc*, Journal of Structural Chemistry, Vol.51, No.5, p.824-832, 2010
- b) **Kitap:** Christie John Geankoplis. *Transport Processes and Separation Process Principles*. Fourth Edition, Prentice Hall, p.386-398, 2002
- c) **Kongre:** Sadychov F.S., Aydin C., Ahmedov A.İ. Application of Information-Communication Technologies in Science and education. II International Conference. "Higher Twist Effects In Photon- Proton Collisions", Baku, 01-03 Noyabr, 2007, ss 384-391

Kaynakların büyüklüğü 9 punto olmalıdır.

9. **Sayfa ölçüleri;** üst: 2.8 cm, alt: 2.8 cm, sol: 2.5 cm, sağ: 2.5 cm şeklinde olmalıdır. Metin 11 punto büyütükte **Palatino Linotype** fontu ile ve tek aralıkta yazılmalıdır. Paragraflar arasında 6 puntoluk yazı mesafesinde olmalıdır.
10. Orijinal araştırma eserlerinin tam metni 15 sayfadan fazla olmamalıdır.
11. Makaleler dergi editör kurulunun kararı ile yayımlanır. Editörler makaleyi düzeltme için yazara geri gönderebilir.
12. Makalenin yayına sunusu aşağıdaki şekilde yapılır:
 - Her makale en az iki uzmana gönderilir.
 - Uzmanların tavsiyelerini dikkate almak için makale yazara gönderilir.
 - Makale, uzmanların eleştirel notları yazar tarafından dikkate alındıktan sonra Derginin Yayın Kurulu tarafından yayına sunulabilir.
13. Azerbaycan dışından gönderilen ve yayımlanacak olan makaleler için,(derginin kendilerine gönderilmesi zamanı posta karşılığı) 30 ABD Doları veya karşılığı TL, T.C. Ziraat Bankası/Üsküdar-İstanbul 0403 0050 5917 No'lu hesaba yatırılmalı ve makbuzu üniversitemize fakslanmalıdır.

ПРАВИЛА ДЛЯ АВТОРОВ

1. «Journal of Baku Engineering University» - Физика публикует оригинальные, научные статьи из области исследования автора и ранее не опубликованные.
2. Статьи принимаются на английском языке.
3. Рукописи должны быть набраны согласно программы **Microsoft Word** и отправлены на электронный адрес (journal@beu.edu.az). Отправляемые статьи должны учитывать следующие правила:
 - Название статьи, имя и фамилия авторов
 - Место работы
 - Электронный адрес
 - Аннотация и ключевые слова
4. **Заглавие статьи** пишется для каждой аннотации заглавными буквами, жирными буквами и располагается по центру. Заглавие и аннотации должны быть представлены на трех языках.
5. **Аннотация**, написанная на языке представленной статьи, должна содержать 100-150 слов, набранных шрифтом 9 punto. Кроме того, представляются аннотации на двух других выше указанных языках, перевод которых соответствует содержанию оригинала. Ключевые слова должны быть представлены после каждой аннотации на его языке и содержать не менее 3-х слов.
6. В статье должны быть указаны коды UOT и PACS.
7. Представленные статьи должны содержать:
 - Введение
 - Метод исследования
 - Обсуждение результатов исследования и выводов.
 - Если ссылаются на работу на русском языке, тогда оригинальный язык указывается в скобках, а ссылка дается только на латинском алфавите.
8. **Рисунки, картинки, графики и таблицы** должны быть четко выполнены и размещены внутри статьи. Подписи к рисункам размещаются под рисунком, картинкой или графиком. Название таблицы пишется над таблицей.
9. **Ссылки** на источники даются в тексте цифрой в квадратных скобках и располагаются в конце статьи в порядке цитирования в тексте. Если на один и тот же источник ссылаются два и более раз, необходимо указать соответствующую страницу, сохраняя порядковый номер цитирования. Например: [7, стр.15]. Библиографическое описание ссылаемой литературы должно быть проведено с учетом типа источника (монография, учебник, научная статья и др.). При ссылке на научную статью, материалы симпозиума, конференции или других значимых научных мероприятий должны быть указаны название статьи, доклада или тезиса.

Например:

- a) **Статья:** Demukhamedova S.D., Aliyeva I.N., Godjayev N.M. *Spatial and electronic structure of monomeric and dimeric complexes of carnosine with zinc*, Journal of Structural Chemistry, Vol.51, No.5, p.824-832, 2010
- b) **Книга:** Christie on Geankoplis. *Transport Processes and Separation Process Principles*. Fourth Edition, Prentice Hall, 2002
- c) **Конференция:** Sadychov F.S, Fydin C, Ahmedov A.I. Appligation of Information-Communication Nechnologies in Science and education. II International Conference. "Higher Twist Effects In Photon-Proton Collision", Bakı,01-03 Noyabr, 2007, ss.384-391

Список цитированной литературы набирается шрифтом 9 punto.

10. **Размеры страницы:** сверху 2.8 см, снизу 2.8 см, слева 2.5 и справа 2.5. Текст печатается шрифтом **Palatino Linotype**, размер шрифта 11 punto, интервал-одинарный. Параграфы должны быть разделены расстоянием, соответствующим интервалу 6 punto.
11. Полный объем оригинальной статьи, как правило, не должен превышать 15 страниц.
12. Представление статьи к печати производится в ниже указанном порядке:
 - Каждая статья посыпается не менее двум экспертом.
 - Статья посыпается автору для учета замечаний экспертов.
 - Статья, после того, как автор учел замечания экспертов, редакционной коллегией журнала может быть рекомендована к печати.